DOE-FIU SCIENCE & TECHNOLOGY WORKFORCE DEVELOPMENT PROGRAM

STUDENT SUMMER INTERNSHIP TECHNICAL REPORT

June 7, 2010 to August 13, 2010

Development of a Prototype Methyl-Mercury Monitor for Pore Water Analysis at Oak Ridge Reservation Creek Beds

Principal Investigators:

Charles C. Castello (DOE Fellow)
Florida International University

Thomas G. Thundat, Ph.D., Mentor
Oak Ridge National Laboratory

Acknowledgements:
David Roelant, Ph.D., Director of Research
Applied Research Center, Florida International University

Yong Cai, Ph.D., Professor
Florida International University

Guangliang Liu, Ph.D., Research Associate
Florida International University

Yanbin Li, Ph.D., Postdoctoral Research Associate
Florida International University

Florida International University Collaborator & Program Director:

Leonel Lagos, Ph.D., PMP®

Prepared for:

U.S. Department of Energy
Office of Environmental Management
Under Grant No. DE-FG01-05EW07033

ABSTRACT

This study involves proof-of-concept research for an innovative, low-cost, and portable methylmercury (MeHg) monitor to be utilized at Oak Ridge Reservation (ORR) creek beds. The MeHg monitor comprises three primary steps: (1) chemical separation; (2) preconcentration using the Purge-and-Trap (P&T) method; and (3) sensing using Quartz Crystal Microbalance (QCM) sensors. The study is split into two stages, the first dealing with the measurement of inorganic mercury (Hg) (e.g. Hg^{2+}) and the second with organic Hg (e.g. MeHg). Inorganic Hg was measured using a modified version of the U.S. Environmental Protection Agency's (U.S. EPA) Method 1631, Revision E for chemical separation using stannous chloride ($SnCl_2$) as the derivatization reagent. Preconcentration was handled using a gold trap in the P&T method and Hg was released employing a variable voltage controller and heating coil at 450°C. Organic Hg on the other hand, was quantified using the aqueous phenylation technique for chemical separation using sodium tetraphenylborate ($NaBPh_4$) as the derivatization reagent. Preconcentration was handled using a Tenax trap in the P&T method and Hg was released employing a variable voltage controller and heating coil at 250°C. Sensing in both cases was managed via utilization of QCM sensors functionalized with gold, which causes amalgamation when Hg comes into contact with the gold surface. This causes a change in mass on the sensor's surface, thereby translating to a resonant frequency shift. A variable voltage controller and Pyrolysis coil heated to 800°C was needed to convert organic Hg species to elemental Hg after the Tenax trap which is required for Hg to adsorb to gold when measuring organic Hg. The characteristics of both polished and etched surface QCM sensors were studied in measuring inorganic Hg at different flow-rates (18 mL/min and 50 mL/min). The polished surface QCM sensors resulted with linear ranges of detection of 1 mg/L to 10 mg/L and 1 mg/L to 10 mg/L with regression values of 0.9987 and 0.9736 for 18 mL/min and 50 mL/min respectively. The etched surface QCM sensors resulted with linear ranges of detection of 1 mg/L to 10 mg/L and 1 mg/L to 10 mg/L with regression values of 0.9888 and 0.9864 for 18 mL/min and 50 mL/min respectively. An etched surface QCM sensor with a flow-rate of 18 mL/min was used for organic Hg determination due to having at least 5 times the frequency response compared with other variations. However, the MeHg monitor was unresponsive due to the Hg concentrations that were experimented, ranging between 0 μg/L to 17 μg/L. Regeneration of polished and etched surface QCM sensors was also investigated with microscopic imaging which demonstrated the results. Findings in this study revealed that further investigation of QCM sensors and other alternative sensing technologies are need to determine the viability of the MeHg monitor.

TABLE OF CONTENTS

LIST OF FIGURES

LIST OF TABLES

1. INTRODUCTION

There are many ongoing efforts to develop simple techniques and devices for quick and easy determination of mercury (Hg). These include portable devices such as sensors [1] [2] and probes [3] as well as mobile instrumentation that can be deployed in the field [4] [5]. However, these devices and techniques can rarely be used for methylmercury (MeHg) analysis. In fact, even for total Hg (THg) analysis, these devices and techniques have limited application for environmental samples because the sensitivity of most of these methods is insufficient for detecting environmentally relevant concentrations of Hg. It is more difficult for these methods to be employed for MeHg analysis because (1) MeHg concentration in the environmental matrix (other than in biological samples) is much lower (about 10-100 times lower) than THg; (2) MeHg coexists with inorganic Hg species (which contributes to the dominant fraction of THg); and (3) most of these methods are unable to differentiate MeHg from inorganic Hg. However, MeHg is the most toxic Hg species that can be bioaccumulated into fish through the food chain and then enter the human body through fish consumption. In addition, the mechanisms for the methylation and de-methylation of Hg are not well understood and vary in different ecosystems. Current methods used for MeHg analysis involve field sample collection, sample transport to and storage in the laboratory, sample pretreatment, and instrumental analysis. The disadvantages of these methods include time-consuming, tedious, and sometimes troublesome work in order to preserve and isolate MeHg species from the environmental matrix during sample treatment, which results in the high cost of MeHg analysis of environmental samples. For these reasons, the development of a MeHg monitor for rapid measurement of many samples of pore water in the field at a greatly reduced cost would considerably expand the number and complexity of experiments in Hg contaminated areas, particularly at Oak Ridge Reservation (ORR).

The ORR is owned by the United States Department of Energy (U.S. DOE) which is located in Oak Ridge, Tennessee. ORR was established in the early 1940s as part of the Manhattan Project, which helped produce materials for the first atomic bomb. Throughout the following years, many changes have occurred at ORR to help meet U.S. needs in defense, energy, and research. There are currently three major operating sites: Oak Ridge National Laboratory (ORNL), East Tennessee Technology Park (formerly the K-25 Site), and the Oak Ridge Y-12 National Security Complex [6], where Y-12 is the major area of concern as this facility formally produced components for various nuclear weapons systems in the 1950s and early 1960s. Hg was used at Y-12 as a key element to capture enriched lithium by separating lithium isotopes. As a result, Hg has become a key contaminant in soil, sediment, surface water, ground water, buildings, drains, and sumps [7] throughout ORR. Research results have discovered that concentrations of Hg in Upper East Fork Poplar Creek (EFPC) watershed (soil) range from 0.01 to 7,700 mg/kg [8]. Measurements taken at EFPC sediments and Lower Poplar Creek show Hg peaking at 40 mg/kg (depth of 10-20 cm) and 15 mg/kg (depth of 40-60 cm) [9]. Measured values of Hg concentrations are much greater than U.S. Environmental Protection Agency's (U.S. EPA's) standard of 1 mg/kg [10]. This large amount of Hg has the potential of converting to MeHg through the methylation process which poses a serious issue at ORR. This makes it imperative to find a quick and easy technique of measuring MeHg.

The development of such a technique will not be an easy task due to the extremely low concentration of MeHg in the environment (approximately 10-13 M in natural waters). In order to detect MeHg, the method/technique used must (1) employ the use of a Hg detector (e.g. Atomic Fluorescence Spectroscopy (AFS) or various sensors) with a relatively low detection limit; and (2) be selective toward MeHg rather than inorganic Hg species (or these Hg species are separated in a separate step). Since the sensitivity of currently available instruments or sensors is insufficient for direct measurement of MeHg in environmental samples, a preconcentration step is usually needed.

This project will develop an innovative, low-cost, and portable Hg monitor platform that will measure MeHg in water in the field. The proposed technique will involve three key steps: 1) chemical separation using a derivatization reagent; 2) preconcentration using on-line purge-and-trap (P&T); and 3) detection using Quartz Crystal Microbalance (QCM) sensors. This approach exploits the proven high preconcentration factor and effective cleanup associated with the chemical separation techniques employed in this study and followed by P&T concentration. QCM sensors yield a significant resonant-frequency shift as its loading mass is subjected to a small change. QCM sensors are simply functionalized with gold, which efficiently adsorbs Hg^0 (elemental Hg).

The rest of this document is organized as follows:

- Section 2 - Executive summary.
- Section 3 - Background review including:
  - Hg characterization.
  - Importance of measuring MeHg.
  - Traditional methods of quantifying MeHg.
  - Why QCM sensors were chosen.
- Section 4 - Research descriptions including experimental setups.
- Section 5 - Analysis and results generated from the experimental studies.
- Section 6 - Conclusions.

2. EXECUTIVE SUMMARY

The described research work is supported by the DOE-FIU Science and Technology Workforce Development Program, an innovative program developed by the U.S. DOE Office of Environmental Management and FIU's Applied Research Center (ARC) in creating a pipeline of minority students for DOE's future workforce. A DOE Fellow (Charles C. Castello) was sent to Oak Ridge National Laboratory (ORNL) in Oak Ridge, TN for a 10-week internship in the summer of 2010 (June 7 – August 13, 2010). There, the DOE Fellow was mentored by Dr. Thomas G. Thundat in the Biosciences Division, Nanoscale Science and Devices Group. This internship was coordinated by the Applied Research Center at FIU, the Oak Ridge Institute for Science and Education (ORISE), and the Higher Education Research Experience (HERE) Program.

This research aims to develop a proof-of-concept for an innovative, portable, and low cost methylmercury (MeHg) analyzer to improve scientific understanding, risk assessment of Hg contamination, and decision support for MeHg and mercury (Hg) methylation/de-methylation at Oak Ridge Reservation creek beds. This is an extremely important subject due to researchers and scientists not fully understanding the processes of methylation and de-methylation. Current methods used for MeHg analysis involve field sample collection, sample transport to and storage in the laboratory, sample pretreatment and instrumental analysis. The disadvantage of these methods is that they involve time-consuming, tedious, and sometimes troublesome work in order to preserve and isolate MeHg species from the environmental matrix during sample treatment, which results in the high cost of MeHg analysis of environmental samples. For these reasons, the development of a MeHg monitor for rapid measurement of many samples of pore water in the field at a reduced cost would be of great benefit, expanding the number and complexity of experiments in Hg contaminated areas.

3. BACKGROUND

In order to fully grasp the significance of this project, reviews on Hg, the importance of measuring MeHg, traditional methods of measuring MeHg, and why QCM sensors were chosen were performed. Different parameters affecting Hg methylation and de-methylation were also included in these discussions.

3.1 Mercury

Hg, a toxic element present in the environment, is used for a variety of different applications including auto parts, batteries, fluorescent bulbs, medical products, thermometers, and thermostats [11]. It occurs in three oxidation states: Hg(0) (elemental Hg), Hg(I) (Hg^{+}), and Hg(II) (Hg^{2+}), where Hg^{2+} could be converted to MeHg via the methylation process. It should be noted that MeHg is considered approximately 100-1,000 times more toxic to organisms than inorganic species [12]. Exposure to this and other forms of Hg is extremely hazardous to humans and can result in Hg poisoning, which can cause severe neurological disorders. Symptoms include deterioration to the nervous system, impaired hearing, speech, vision and gait. Involuntary muscle movements, skin and mucus membrane corrosion, and difficulty chewing and swallowing can also occur [13]. The risk of Hg poisoning in humans is significantly increased via consumption of exposed fish in which Hg has been bioaccumulated. Bioaccumulation occurs as a result of Hg uptake in small fish and subsequent concentration/biomagnification up the food chain as large amounts of small fish are eaten by larger fish, which are then ultimately consumed by humans. The primary species of fish that act as carriers of Hg include swordfish, shark, and ahi tuna [14].

Another important point to discuss is the Hg cycle which transfers Hg throughout the environment. The first step involves the release of Hg in its gaseous form from rock, soils, water, volcanoes, and human activities [15]. These Hg emissions are then transported through the atmosphere and can be deposited in two forms: dry and wet. Dry deposition is where non-soluble Hg settles from the atmosphere, whereas wet deposition, which takes place more rapidly, occurs through different types of precipitation such as rain and snow. Once deposited, Hg is utilized in a variety of different processes such as sedimentation, bioaccumulation in the food chain, etc. Hg can then be returned to the atmosphere through volatilization and then recycled as described above. The complete Hg Cycle is shown in Figure 1.

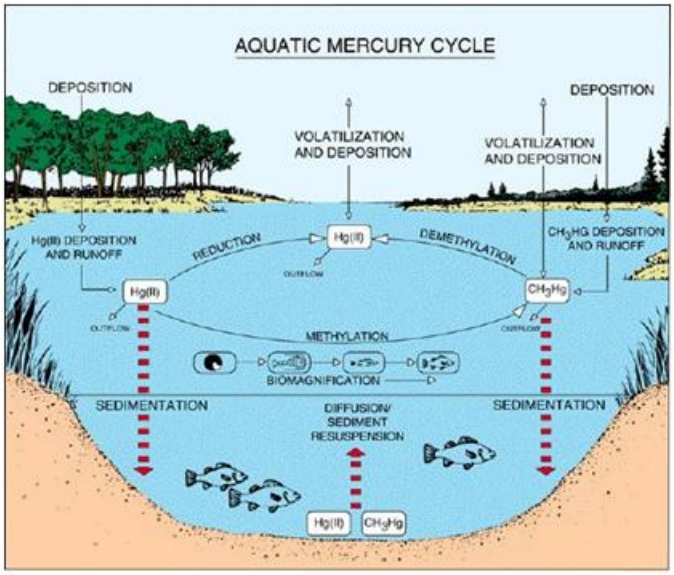

Figure 1 – Mercury cycling [16].

3.2 Why measure MeHg?

There are many parameters that correlate with Hg methylation and de-methylation in the environment that are easily measurable for use in understanding these processes. The two major factors that affect this are microbial activity and the concentration of bio-available Hg (mainly Hg^{2+}), which in turn are affected by a variety of different parameters such as temperature, pH, oxidation-reduction potential (ORP), and the presence of inorganic and organic complexing agents [17]. Measuring the concentrations of Hg^{2+} can be useful in determining the likelihood of methylation and de-methylation due to MeHg being more bioavailable because of its shorter resistance time in the environment [18].

Measuring temperature, pH, and ORP can also be very useful in determining the possibility of Hg methylation and de-methylation. It has been observed in many cases that Hg methylation rates in aquatic systems are largest during the summer months [19,20]. This is due to the overall increase in microbial activity caused by higher temperatures, which in turn increases methylation. It has also been shown in [21,22] that in lower temperatures, de-methylation is favored. pH is also an indicator of Hg methylation and de-methylation. Acidified lakes may be partly to blame for high levels of Hg found in freshwater fish, [23][24] where the concern is that low pH values may lead to the increased production and/or bioaccumulation of MeHg. pH does not directly affect methylation rates, but it does however affect the solubility and mobility of Hg and MeHg which in turn affect the occurrence of methylation. De-methylation rates are also affected by pH levels. A decrease in anaerobic de-methylation in surface sediments has been observed with low levels of water pH [25]. ORP is another indicator parameter which has been proven to occur in both aerobic and anaerobic environments [26][27]. Based on pure culture studies, the methylation process was faster under aerobic conditions. However in natural environments, anoxic sediments and water have been shown to produce the largest rates of methylation, which is now generally accepted as the norm [28][29] due to

the increased activity of anaerobic sulfate-reducing bacteria (SRB), discussed in the following paragraph.

There are other parameters that can be considered when dealing with the likelihood of Hg methylation and de-methylation, such as the concentrations of sulfate (SO_4^{2-}), dissolved oxygen (DO), sulfide (S^{2-}), and salinity. Sulfate in studies has indicated that SRBs are the principal methylators of inorganic Hg in both freshwater and estuarine sediments [30][31][32] where increased activity is affected by anaerobic conditions. Research performed in [33] indicates that low DO levels can favor SRB in Hg methylation. Sulfide concentrations are also useful because studies noted MeHg production is inhibited in soils, sediments, and bacterial cultures due to high levels of sulfides [26][34]. Results from [35] show that MeHg was significantly reduced in fish by adding sulfides such as S^{2-}, iron sulfide (FeS), or iron sulphide (FeS_2) to the aquarium where experiments were taking place. It was also found that dissolved sulfide concentration has an inverse relationship with MeHg production in sediments or sediment porewaters [31][36][37]. This could possibly be due to Hg forming the insoluble species mercury sulfide (HgS) in the presence of sulfide. Results in [34][38] indicate that Hg in its HgS form cannot be utilized to produce MeHg under anaerobic conditions. Salinity can also be used to determine whether an environment is conducive to Hg methylation and de-methylation. This is shown in [39][40] where methylation activity in marine and estuarine sediments is usually lower than that of freshwater sediments due to salinity. It is also stated in [40] that there is a strong inverse relationship between the salinity of anaerobic sediments and Hg^{2+} methylation. Experimental results compiled in [31] show that only 40% of MeHg produced in low-salinity sediments occurred in high-salinity sediments. The effect of salinity on Hg methylation tends to be inhibitive which is pronounced under reducing conditions, while high levels of salinity appear to promote de-methylation [29]. The decrease in MeHg production caused by salinity is due to the microbial production of sulfide from sea salt sulfate. It was mentioned previously there is an inverse relationship between sulfide and Hg methylation.

There are other lesser known parameters which help in determining the likelihood of Hg methylation and de-methylation, such as ammonium (NH_4^+), nitrate (NO_3^-), chloride (Cl^-), and selenium (SeO_3^{2-}) [12][41] concentrations, where NH_4^+ is shown to inhibit microbial activity which in turn decreases methylation and the formation of MeHg [42][43]. NO_3^-, on the other hand, stimulates microbial activity which aids in the formation of MeHg [46]. Cl^- is another indicator reducing the amount of reactive available Hg^{2+}, the lower levels increasing methylation [44]. As for SeO_3^{2-}, research in [45] indicates that the methylation rate of Hg was significantly reduced and the concentration of Hg^{2+} increased due to the presence of Na_2SeO_3. The net formation of MeHg was increased due to a low concentration of Na_2SeO_3 mainly by increasing the concentration of Hg^{2+}. Na_2SeO_3 at high concentrations, however, increased the de-methylation rate of MeHg and reduced the methylation rate of Hg. Figure 2 shows a summary of the relationships between the various indicator parameters discussed.

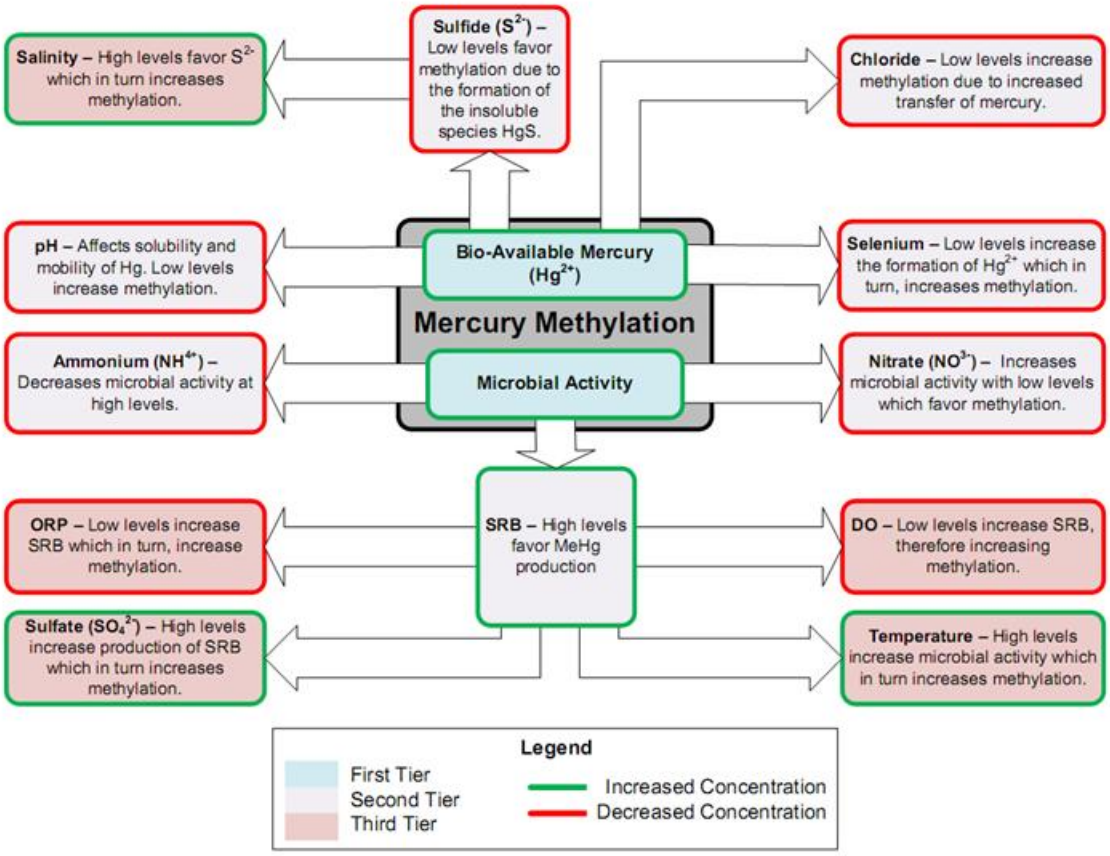

Figure 2 – Parameter relationships for mercury methylation.

The various indicator parameters described are all important in the formation of MeHg through methylation and de-methylation. However, in order to study the relationships between these parameters, a quick and easy quantification of MeHg is extremely important. This will not only reduce the cost of analysis, but also increase the number of experiments that can be accomplished in the field.

3.3 Traditional methods of quantifying Hg

There are currently many techniques available for ex-situ measurement of Hg at a variety of different sensitivity levels such as: (1) Atomic Absorption Spectroscopy (AAS) [46]-[49]; (2) Atomic Emission Spectroscopy (AES) [50]; (3) Atomic Fluorescence Spectroscopy (AFS) [51]; (4) Inductively Coupled Plasma Mass Spectrometry (ICPMS) [52]; (5) Potentiometric Detection (PD) [53]; and Voltammetric Detection (VD) [54]. Shown below are various reviewed papers based on the abovementioned techniques.

3.3.1. Atomic Absorption Spectroscopy

A method using cold-vapor atomic absorption was presented in [46]. This technique utilizes an ordinary 4-cm UV-cell for Hg detection. Hg^{2+} is reduced and then partitioned into aqueous and gas phases in a stoppered UV-cell. A direct atomic absorption measurement is taken when a Hg resonant light beam passes through the vapor phase of

the system while non-atomic absorption is corrected using an automatic background corrector. The obtained calibration graph for Hg^{2+} in 4M of sulfuric acid (H_2SO_4) shows linearity between 0 and 30 μg/L and absorbance at concentrations up to 50 μg/L, where a slight deviation is apparent from linearity. The detection limit was found to be 0.02 μg/L, where absorbance was found to be dependent on the concentration of sulfuric acid.

A technique for measuring the speciation of Hg was developed in [47] and was applied to determine ng/L concentrations of methyl- and inorganic Hg in Lake Constance, Germany. The separation of Hg species is accomplished using Gas Chromatography (GC) of derivatized Hg species on a wide bore capillary column. The solvent is then vented using a bypass valve and the separated Hg species are pyrolysed on-line at $800^{O}C$ for production of Hg atoms which is detected using AAS at the 253.7 and 184.9 nm lines simultaneously in a quartz cuvette. The use of the 184.9 nm line provides a more than five-fold increase in sensitivity compared with the conventional 253.7 nm line and an absolute detection limit of 0.5 pg of Hg.

AAS is used by Szkoda et al. [48] to determine the THg in tissue, animal organs, and milk. A detailed process is explained for sampling, calibration, and analysis where the Advanced Mercury Analyzer (AMA) 254 spectrometer was tested in order to determine the influence of instrumentation on Hg level changes in different biological samples. The working range of this technique is 0.002–0.500 mg/kg with a detection limit of 0.0004 mg/kg.

Detection of Hg [49] was also accomplished by using Headspace Solid Phase Microextraction (HS-SPME) coupled with Electrothermal AAS (ETAAS). A gold wire is mounted in the headspace of a sample solution which is sealed in a bottle. The wire is used to collect Hg vapor generated by the addition of sodium tetrahydroborate ($NaBH_4$). The gold wire is then inserted into a graphite furnace of an ETAAS instrument. By applying an atomization temperature of $600^{O}C$, Hg is rapidly desorbed from the wire and determined with high sensitivity. Factorial design and response surface analysis methods were also studied for optimization of the effect of five different variables in order to maximize the Hg signal. The detection limit of this method is 0.006 ng/mg.

3.3.2. Atomic Emission Spectroscopy

A method with a sensitivity of 0.01 ng/L for Hg detection in natural waters using atmospheric pressure Helium Microwave Induced Plasma (He-MIP) emission spectroscopy was presented in [50]. Hg vapor was generated from water samples by reduction and purging, and was collected with a gold amalgamation trap. The Hg vapor is then removed from the trap with heat and introduced into the He-MIP. The atomic emission line of 253.7 nm was used for the determination of Hg.

3.3.3. Atomic Fluorescence Spectroscopy

An analytical procedure was studied [51] based on GC AFS following aqueous phenylation with $NaBPh_4$ for determining MeHg and ethylmercury (Ethyl-Hg) compounds in fish and sediment samples. Advantages of this technique are its ability to derive products in the aqueous phase. Ethyl-Hg and inorganic Hg species can be detected with high sensitivity and high selectivity.

3.3.4. Inductively Coupled Plasma Mass Spectrometry

A novel technique was developed in [52] for detecting Hg methylation rates in sediments. This is accomplished using an ICPMS instrument to measure individual isotopes. This instrument is used to detect MeHg compounds after separation by GC. MeHg is isolated from sediments by distillation, converted to methylethylmercury by sodium tetraethylborate ($NaBEt_4$), and analyzed after P&T pre-collection on a Tenax adsorber and thermodesorption onto the GC column. Detection limits are ≈ 1 pg (as Hg) absolute or 0.02 ng/g dry sediment.

3.3.5. Potentiometric Detection

A small Hg ion selective electrode was demonstrated in [53], which is responsive to changing halide concentrations which are interpretable as Hg halide speciation in solution. Electrodes consist of a composite, conductive epoxy, and an insoluble salt of the species to be detected.

3.3.6. Voltammetric Detection

Hg detection in urine samples was accomplished in [54] by using differential pulse stripping voltammetry. Hg in the samples was oxidized to Hg^{2+} using bromine (Br) and potassium permanganate ($KMnO_4$). Hg^{2+} was reduced by sodium tetrahydroborate ($NaBH_4$) to the metallic state and volatized using N_2 as the carrier gas. Gas containing Hg vapor was then dried and accumulated on a gold plated impregnated graphite electrode. The stripping process was performed from 0.1M $HClO_4$ + $3x10^{-3}$M HCl solution. Operating range was from 1 to 10 µg/L and the detection limit was 0.4 µg/L of Hg.

3.4 Why choose QCM Sensors?

A survey on the various sensors involved with in-situ measurement of Hg concentrations was reviewed. The assorted sensor technologies could be separated into six categories including: (1) biosensors / chemical sensors; (2) conductometric sensors / thin film technology; (3) in vivo monitoring Hg; (4) microcantilever sensors; (5) nanosensors; and (6) surface acoustic wave (SAW)-based sensors/piezoelectric detection. A summary of the different types of sensors, fabrication difficulties, and detection limits is shown in Table 1. The review shows that QCM sensors (i.e. SAW sensors) were chosen because of their detection limit (10^{-8} M), cost, and ease of implementation. QCM sensors have also been widely researched and utilized in the industry which explains its commercial availability.

Table 1 – A Comparison of Different Types of Hg Sensors [55]

Type of Sensor	*Sensing Principle*	*Fabrication of the Sensor*	*Forms of Mercury Detection*	*Detection Limit*	*References*
Biosensor	Mercury interaction with bacterial cell	Moderately Difficult	Inorganic Hg and Organic Hg	~ 10^{-7} M	[94]
	Mercury interaction with antibody	Moderately Difficult	Hg^{2+}	~ 10^{-6} M	[89]
Chemical Sensor	Fluorescence Quenching	Moderately Difficult	Hg^{2+}	~ 10^{-6} M	[58]
	Fluorescence Enhancing	Moderately Difficult	Hg^{2+}	~ 10^{-9} M	[59]-[61]
Conductometric Sensor	Conductivity/ Resistance	Easy	Hg Vapor	~ 10^{-8} M	[66][69][90]
Microcantilever Sensor	Physical Property Changes	Easy	Hg^{2+}, Hg^{0}	~ 10^{-11} M	[74][75][78]
SAW Sensor	Oscillation Frequency	Easy	Hg Vapor	~ 10^{-8} M	[81]
Piezoelectric Sensor	Frequency of Vibration	Easy	Hg^{0}	~ 10^{-9} M	[85][86]
Nanosensor	Interaction with Nanoparticles	Moderately Difficult	Hg^{2+}	10^{-11} ~ 10^{-15} M	[72][91]

3.4.1. Biosensors / Chemical Sensors

Biosensors for the detection of Hg in soils were developed which include protein-based, whole bacterial cell-based, and plant-based [56]. Protein biosensors use the fusion protein GST-SmtA. A thioctic acid monolayer was self-assembled on a well-cleaned gold electrode and the protein was coupled via covalent carbodiimide coupling. Capacitance was measured by applying a potential pulse of 50mV and recording the current transients. The whole cell biosensor was constructed based on lux genes from Vibrio fischeri which were fused to a Hg-inducible mer gene and introduced into the Escherichia coli (CM2624). The resulting strain emitted light in the presence of Hg ions. Bioluminescence was measured after 5 hours of incubation which could be considered a drawback. Lastly, a plant sensor was developed to evaluate potential soil phytotoxicity using a bioassay including several morphological and biochemical parameters. Findings for all three of these sensors indicate that the whole bacterial cell and protein biosensors successfully detected Hg concentration in soil with responses comparable to AAS. Also, due to limited uptake of Hg by plants, the plant sensor appears to be a poor indicator for Hg in soils.

Research in [57] deals with the use of a Hg bioluminescent bacterial biosensor. An *Escherichia coli* strain was genetically altered to produce firefly luciferase in proportion to its exposure to bioavailable Hg^{2+}. The first part of the research deals with developing and analyzing an analytical protocol. The second phase of the research manipulates Hg^{2+} speciation by the addition of inorganic and organic ligands and the bioavailabilities of the species formed.

A new chemical sensor for the determination of ionic Hg is based on the fluorescence quenching of a sol-gel membrane [58]. The membrane worked according to an ion-exchange mechanism in which Hg^{2+} is bound to a porphyrin immobilized on a sol-gel membrane. The binding of Hg^{2+} quenched the fluorescence signal of the porphyrin; therefore, the change in fluorescence intensity was proportional to the Hg concentration.

Target-induced fluorescence sensors are studied in [59] which are generally based on Hg^{2+} desulfurization reactions, such as cyclizations, hydrolysis, and elimination reactions. The Hg^{2+} promoted desulfurization reaction of a thiocarbazone derivative yields a cyclic product, upon which a fluorescence enhancement is generated. Interference analysis for other cations reveals a specific interaction between the thiocarbazone derivative and Hg^{2+}.

A chemical sensor combined with a flow injection system can continually measure Hg in the environment which is shown in [60]. For example, a sensor based on a non-ion exchanging solid support with thiamine was developed to selectively and sensitively determine ionic Hg. The principle of the method was the oxidation of thiamine to fluorescent thiochrome. The Hg induced fluorescence signal was proportional to the Hg concentration.

The design of fluorescence markers upon the addition of Hg^{2+} is discussed in [61] for Hg^{2+} which is based on a phosphane S^{2-} derivative. The detection limit of 3.8×10^{-9} M was achieved while retaining a high selectivity over competing cations in an aqueous medium. Selective chemodosimeters for Hg have been developed in [1] where Hg-triggered intra-molecular cyclizations of thioureas result in the formation of highly fluorescence molecules. Other fluorescence markers with attached receptors specific to ionic Hg exhibit an enhanced fluorescence upon the addition of Hg^{2+} [62]-[64]. Thiamine (Vitamin B1) acts as a "turn-on" fluorescent marker specific to ionic Hg. As Hg interacts with thiamine, thiamine is oxidized to thiochrome, and Hg is reduced to Hg^0. Overall, fluorescence sensors offer a selective and sensitive approach for the determination and monitoring of Hg in aqueous medium [63].

3.4.2. Conductometric Sensors / Thin Film Technology

A miniaturized Hg sensor was developed in [65] based on thin film technology where amalgam forms when Hg comes into contact with a thin gold film. This effect can be used to determine the presence and concentration of Hg steam which is measured by the change in resistance in the gold caused by the amalgam formation. The regeneration process is accomplished by heating the gold layer to approximately $150^{O}C$ using an electrical heater underneath the gold layer. Elemental Hg vapor is measured in [66] by using two gold films, one as a sensor and the other as a reference. The gold film of the

sensor produces a change in resistance once elemental Hg makes contact. Aluminum films are used to extract Hg from a carrier gas, normally air filtered through activated charcoal. There are two possibilities discussed where the sample can be introduced into the carrier gas: solid or vapor. The limit of detection of the prototype instrument is 0.05 ng of Hg.

Electrical sensors using a silicon substrate deposited with thin gold films were developed in [67] to sense Hg vapor. Hg concentration and exposure time were changed through the experimentation where chemical composition and morphology of the exposed films were studied by X-ray Photoelectron Spectroscopy (XPS), Secondary Ion Mass Spectroscopy (SIMS), Scanning Auger Microscopy (SAM), and Secondary Electron Microscopy (SEM). In samples exposed for a short time, Hg was adsorbed by a thin surface sublayer of gold film. In the case of long exposures, the transformation of the uniform gold film to a dendritic-like coalesced AuHg amalgam occurred.

The adsorption mechanisms of Hg on gold and silver substrates were studied in [68] by exposing the thin film to gaseous metallic Hg, while the Hg concentration, substrate temperature, and exposure length were varied. The resulting changes in the surface morphology of the substrates were studied with Scanning Tunneling Microscopy (STM). The results showed that the collection efficiency of single-crystalline surfaces is a function of both Hg concentration and temperature.

Lastly, various technologies in [69] for measuring Hg vapor in the air have been reviewed for potential use in monitoring the breathing atmosphere of the crew cabin in a National Aeronautics and Space Administration (NASA) spacecraft. Materials tested for Hg sensing include polymer-carbon black composite films with amines in the polymer structure, gold films, gold islands on polymer films, and sintered palladium(II) chloride ($PdCl_2$) films.

3.4.3. In Vivo Monitoring Mercury

In order to determine the Hg concentration, amalgamation with a thin layer of silver is used in [70], which comes into contact with an ionic solution of Hg. Subsequently, a traditional Total-Reflection X-Ray Fluorescence (TXRF) is performed. The second method involves forming an amalgam of gold using microlitre quantities of the solution to be analyzed. TXRF is also performed for determination. The sensitivity of this method is 5 μg/L.

A new sensor for detecting Hg^{2+} ions in aqueous solution has been developed in [71] using new Gold-Nano Particles (AuNP). Rhodamine B (RB) molecules that are highly fluorescent in bulk solution lose fluorescence when adsorbed onto AuNP surfaces as a result of fluorescence resonance energy transfer and collision with AuNPs. In the presence of metal ions such as Hg^{2+}, RB molecules are released from the AuNP surface and thus restore the florescence of RB. The entire detection of Hg^{2+} using this methodology takes 10 min. Selectivity has been improved by modifying the AuNP surfaces with thiol ligands and adding a chelating ligand to the sample solutions. The limit of detection was calculated as 2.0 μg/L.

AuNPs using Rhodamine 6G (Rh6G) were developed in [72] for detecting Hg^{2+} in aqueous solution. Water-soluble and mono-disperse AuNPs have been prepared facilely and further modified with Thio Glycolic Acid (TGA). Free Rh6G dye was strongly fluorescent in bulk solution. The sensor system composing of Rh6G and AuNPs fluoresce weakly as a result of Fluorescence Resonance Energy Transfer (FRET) and collision. The fluorescence of the Rh6G and AuNPs-based sensor was gradually recovered due to Rh6G units departing from the surface of functionalized AuNPs in the presence of Hg^{2+}. Based on the modulation of fluorescence quenching efficiency of Rh6G-AuNPs by Hg^{2+} at pH 9.0 of teraborate buffer solution, a simple, rapid, reliable, and specific turn-on fluorescent assay for Hg^{2+} was proposed. Under optimal conditions, the fluorescence intensity of the sensor is proportional to the concentration of Hg^{2+}. The calibration graphs are linear over the range of $5.0x10^{-10}$ to $3.55x10^{-8}$ mol/L, and the corresponding limit of detection is as low as $6.0x10^{-11}$ mol/L.

3.4.4. Microcantilever Sensors

Gold-coated silicon cantilevers are used to measure Hg vapor in [73]. This is done by using two types of commercial Atomic Force Microscope (AFM) cantilevers (small, ≈ 140 μm × 40 μm × 4 μm; large, ≈ 245 μm × 50 μm × 7 μm), which differ by physical dimensions and surface finish. Each AFM cantilever is coated with a 10 nm film of gold. Results show that the larger of the two AFM cantilevers has a lower sensitivity by 10 times. It is also shown that Hg can be stripped from the gold coating by heating to $350^{O}C$, which would allow the cantilevers to be regenerated and reused.

A Hg vapor detector is researched in [74] based on the use of a microcantilever with an integrated piezoelectric film. The benefit of using this technology is that the cantilever is self-sensing and self-actuating, and therefore does not need alignment of an external optical detection system. When Hg vapor is adsorbed onto gold film on the cantilever, this causes stiffness, and therefore causes the natural frequency of the cantilever to increase due to Hg-gold amalgamation. This shift is detected using the piezoelectric portion of the cantilever in conjunction with a bridge circuit and amplifier. A Hg concentration of 93 ng/L in nitrogen was detected.

The detection of Hg^{2+} in liquids is researched in [75] based on the use of gold coated microcantilevers. The microcantilever undergoes bending due to the accumulation of Hg^{2+} on the gold surface. Light is reflected off the microcantilever to determine the bend which occurs due to the attachment of Hg on the gold. The selectivity of the Hg^{2+} sensor could be improved by coating the gold surface of the microcantilever with a self-assembled monolayer of a long-chain thiol compound.

An electromagnetically actuated resonant cantilever gas sensor system is developed in [76] which features a piezoresistive readout by means of stress-sensitive Metal-Oxide-Semiconductor (MOS) transistors. The monolithic gas sensor system includes a polymer-coated resonant cantilever and the necessary oscillation feedback circuitry, both monolithically integrated on the same chip. The fully differential feedback circuit allows for operating the device in self-oscillation with the cantilever constituting the frequency-determining element of the feedback loop.

The interfacial stress changes at electroactive self-assembled monolayers are investigated in [77] by monitoring the potential-induced deflection of gold coated microcantilevers modified with 12-ferrocenyl-1-dodecanethiol in aqueous perchloric acid solution. Oxidation of the surface-bound ferrocene generates a compressive surface stress which results in the cantilever bending away from the film-coated gold surface.

Oscillating silicon nitride (N_4Si_3) microcantilevers coated with a thin gold film have been utilized in [78] to detect Hg vapor in the air. The cantilever resonance frequency changes to surface mass loading as a result of adsorption of Hg vapor. Furthermore, cantilever bending is also altered due to changes in surface stress induced by Hg adsorption on the gold overlayer. Both of these phenomena can be used to quantitatively detect adsorbed vapors with pg mass resolution.

Adsorption and absorption-induced stresses using microcantilever sensors is investigated in [2]. This is accomplished by studying the interaction between vapor and thin film adsorbed on one side of a biomaterial microcantilever which produces differential stress, resulting in readily measurable curvatures of the cantilever structure. There are two types of gas-solid interaction systems studied: (1) bulk-like absorption and (2) surface-like adsorption. The absorption of hydrogen (H) into palladium (Pd) results in film expansion where the magnitude is governed by H partial pressure. The bending of a biomaterial microcantilever (Pd/Si) due to H absorption depends on the thickness of the Pd film and is reversible, but rate is limited by the surface barrier. In contrast, the stress induced by adsorption of Hg onto a biomaterial (Au/Si) cantilever is irreversible at room temperature, is rate limited by surface coverage, and is independent of the gold-film thickness.

3.4.5. Nanosensors

Nanoelectrode arrays (NEA) based on low-site density carbon nanotubes (CNT) are utilized in [79] to detect trace heavy metal ions. The CNTs-NEAs are coated with a bismuth film for VD of trace Cd(II) and Pb(II) at the sub-ng/L level. The detection limit of 0.04 µg/L was found through optimal experimental conditions. A novel oligo-T-based gold nanoprobe is developed in [3] for rapid and portable detection of Hg^{2+} using a power-free Poly(DiMethylSiloxane) (PDMS) micro fluidic device. This device can be used for rapid and visual detection of low micro molar Hg^{2+} in real environmental samples. Lastly, gold nanowires are utilized in [80] for the electrical detection of Hg^0 and ionic Hg. This is accomplished by monitoring changes in resistance upon exposure to Hg vapor. Concentrations as low as 5 µg/L were detected. Similarly mercury chloride ($HgCl_2$) was used in an aqueous solution as a source for Hg ions and Hg^{2+} was detected at concentrations as low as 10^{-8} M.

3.4.6. SAW-Based Sensor Piezoelectric Detection

A dual delay line SAW sensor was developed in [81] for gaseous Hg by using the interaction between a gold film and Hg, which forms amalgam. The resulting increase in film mass is manifested as a decrease in oscillation frequency. Responses of this sensor to gaseous Hg concentrations are in the µg/L range. Acoustic Plate Mode (APM) microsensors are studied in [82] which are capable of detecting relevant concentrations of aqueous Hg while withstanding typical environmental conditions. This piezoelectric

sensor protects the electronics from potentially corrosive aqueous fluids in the environment while providing significant interaction with the fluid. Gold films are employed to accumulate Hg via surface amalgamation. The added mass is measured as a change in the resonant frequency of the piezoelectric element.

SAW chemical sensors based either on gallium arsenide (GaAs) or gallium nitride (GaN) structures are presented in [83] to measure low concentrations of gaseous Hg. Described is the design of the acoustic part of the sensor, including the structure for the generation and reception of the SAW and the chemo-selective coating made of gold. The technological process to create the device is carried out at a frequency of 250 MHz.

A quartz resonator is used in a piezoelectric sorption sensor [84] to determine the concentration of Hg vapor in the air. A maximum sensitivity of $3x10^{-6}$ g/m^3 can be attained. A built-in microheater is also used with the quartz resonator to regenerate the sensor without dismounting it from the equipment. The temperature used for regeneration is $150^{O}C$.

Gold-coated piezoelectric crystals without substrates were initially tested in [85] to measure the concentration of Hg vapor using three generation techniques to produce standardized vapors: (1) saturation; (2) syringe dilution; and (3) use of a permeation tube. Later, using a permeation tube as a source of metal, some substances were investigated as possible substrates capable of interaction with Hg vapor. The best material found was a mixture of Pd(II) chloride solution (saturated in acetone) and tetrahydroxyethyl-ethylenediamine (THEED) in acetone.

An automatic micro gravimetric screening system based on piezoelectric detection and the use of acidic $SnCl_2$ as a reductant was developed in [86] for the fast detection and determination of total Hg in water. Reduced Hg is detected as an amalgam by using a gold-coated piezoelectric crystal, the sensor subsequently being regenerated by passing it through a peroxydisulfate solution. The detector exhibits good sensitivity, allowing the determination of Hg at sub- μg/L concentration levels (0.30 – 1.00 μg/L).

4. RESEARCH DESCRIPTIONS

There are three key steps in creating an integrated process for measuring MeHg concentrations (i.e. developing a MeHg monitor). These include: (1) Derivatization; (2) preconcentration using the P&T method; and (3) sensing using QCM sensors. Gold is used to functionalize the sensor where amalgamation causes the Hg to bond to the gold surface. This causes a change in mass, thereby translating to a resonant frequency shift. The project was split into two experimental stages: Stage #1 - for measuring inorganic Hg (e.g. Hg^{2+}) and Stage #2 - for measuring organic Hg (e.g. MeHg). The regeneration of QCM sensors was also studied by using a micro-heater, which is described in this section.

4.1 Stage #1 Experiment

Figure 3 displays the initial experimental setup to quantify inorganic Hg. The setup measures the concentration of Hg^{2+} in water. U.S. EPA's Method 1631 was employed to analyze the Hg^{2+} which was reduced to Hg^0 by utilizing $SnCl_2$ in acidic solution. Hg^0 was then purged from the solution in the bubbler using N_2 gas at 350 mL/min for 20 min and trapped on a gold trap. The Hg^0 was released from the trap by heating to 450^{O}C for 10 minutes using a heating coil connected to a variable voltage controller. Hg^0 vapor then travels to the QCM flow cell where different flow rates were tested (18 and 50 mL/min). Initially, different concentrations of $HgCl_2$ were utilized to determine a calibration curve (0, 1,000, 2,000, 5,000, and 10,000 µg/L). Resonant frequency shifts were monitored using an oscillator chip, frequency counter, General Purpose Interface Bus (GPIB), and Personal Computer (PC) with Laboratory Virtual Instrumentation Engineering Workbench (LabVIEW). These experiments were repeated using both polished and etched surface QCM sensors to determine which type produced better results. All chemical and material information utilized throughout this project can be found in Appendix A.

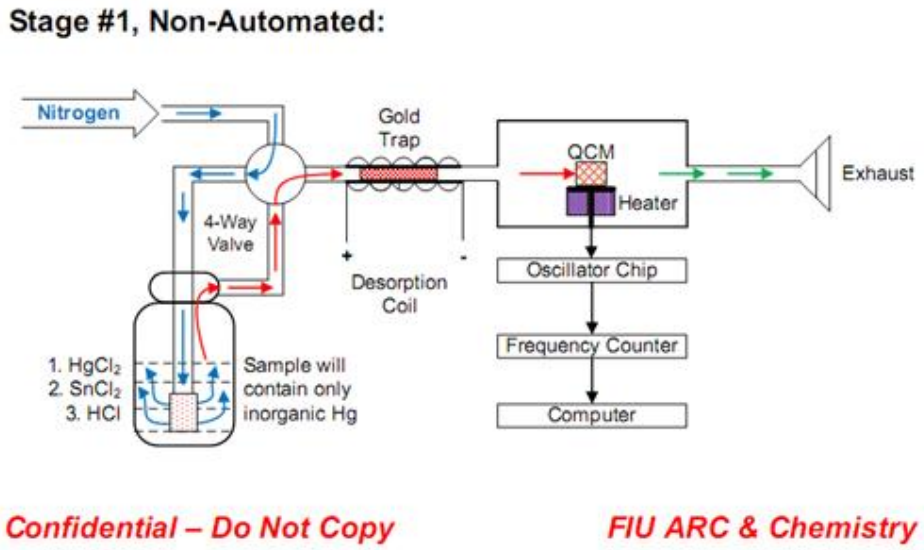

Figure 3 – Stage #1 of MeHg experimental plan.

4.1.1. Determining Hg^{2+} Concentration using EPA's Method 1631

The experimental setup of instruments for Stage #1 is shown in Figure 4 which used EPA's Method 1631 Revision E [87]. This was accomplished by mixing 100 mL of deionized (DI) water, 0.5 mL of $SnCl_2$ solution, and 100 mg/L of $HgCl_2$ standard needed for the experiment in a 200 mL bubbler. The solution was then purged at 350 mL/min with N_2 for 20 minutes and Hg^0 was transferred into a gold trap shown in Figure 5. The gold trap was then heated to 450°C for 5 minutes using a heating coil connected to a variable voltage controller from Starco Energy Products Company (Model # 3PN1010B), exhibited in Figure 6. During this time, N_2 gas was flowing at either 18 or 50 mL/min to transport the inorganic Hg being released by the gold trap to the QCM sensor.

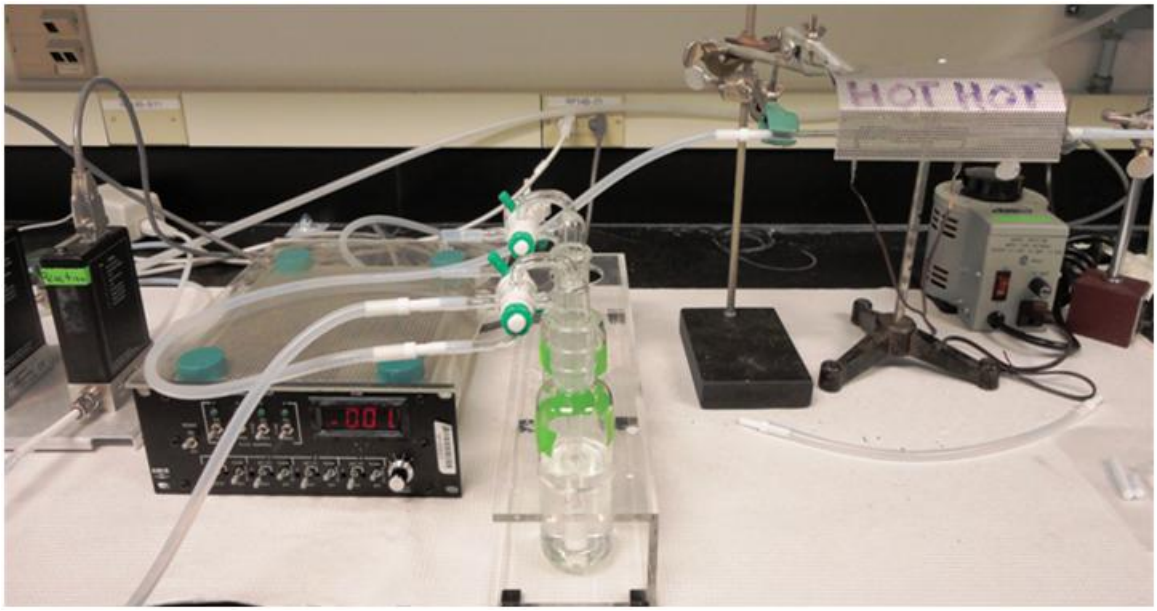

Figure 4 – Experimental setup of Stage #1 (Chemical Separation).

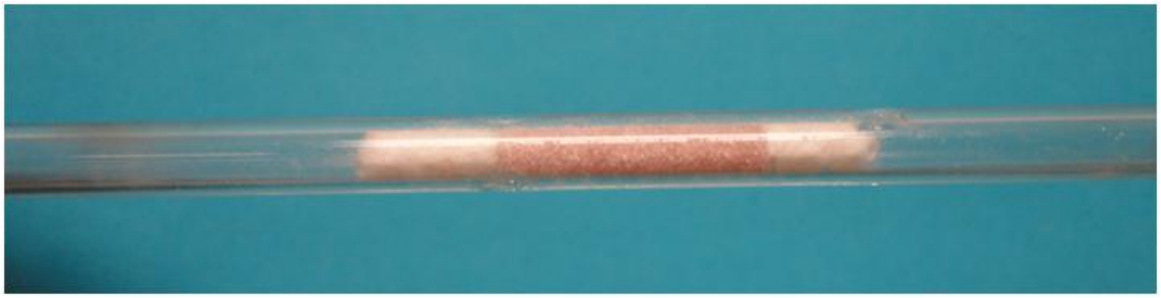

Figure 5 – Gold trap in P&T method.

Figure 6 – Staco Energy Products Company variable voltage controller.

4.1.2. Sensing using QCM Sensors

The experimental setup of the sensing aspect of this project was accomplished using a QCM sensor, presented in Figure 7. The QCM sensors utilized in this project were purchased from International Crystal Manufacturing (ICM) Company, Inc. All had a resonant frequency of 10 MHz with polished and etched surfaces. An example of the etched surface QCM sensor is shown in Figure 8. The flow-cell used in these experiments was also from ICM and was a static cell (ID # 35368) made of Teflon. The same flow-cell plus slight modifications is shown in Figure 9, which was modeled in SolidWorks 3D Computer-Aided Design (CAD) Software.

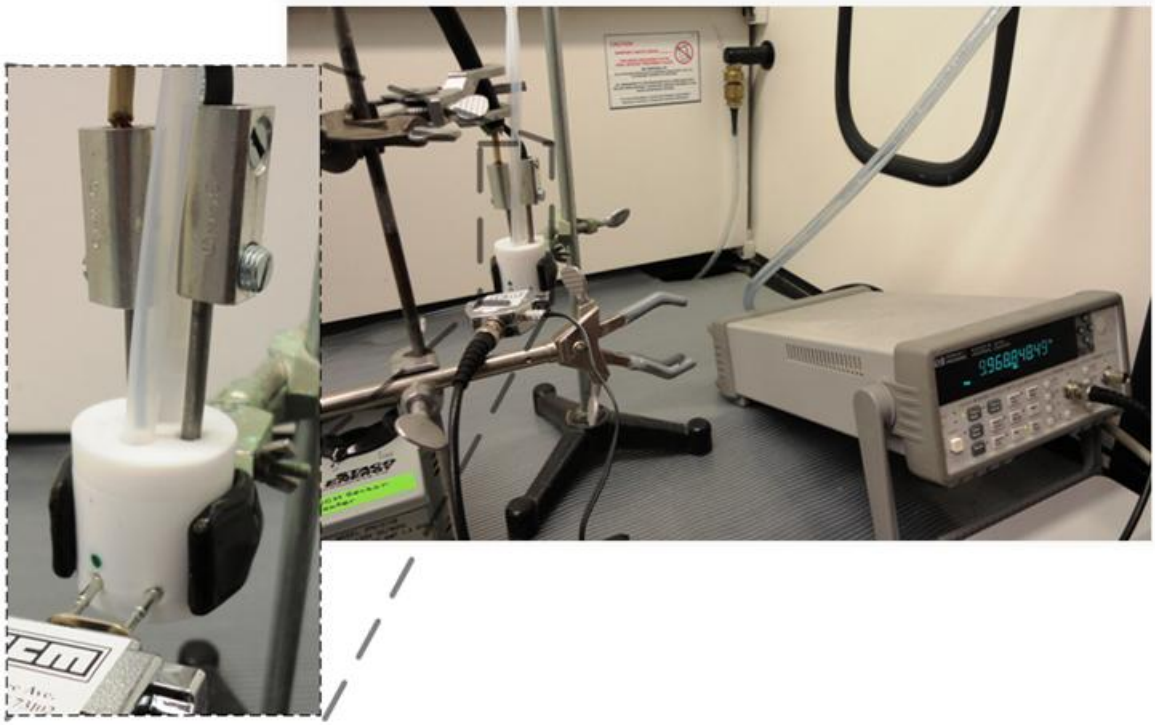

Figure 7 – Experimental setup of Stage #1 (Sensing).

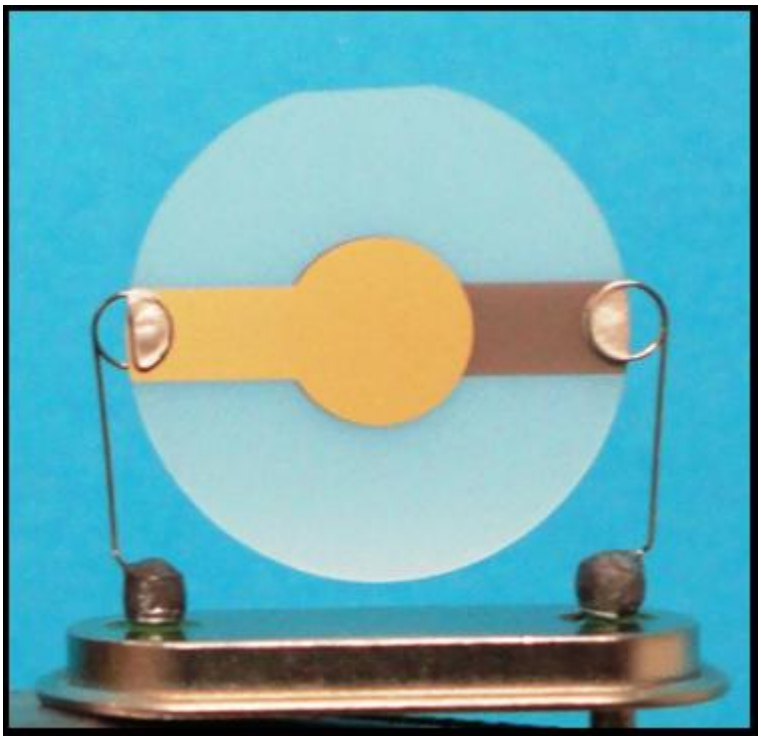

Figure 8 – Etched surface QCM sensor.

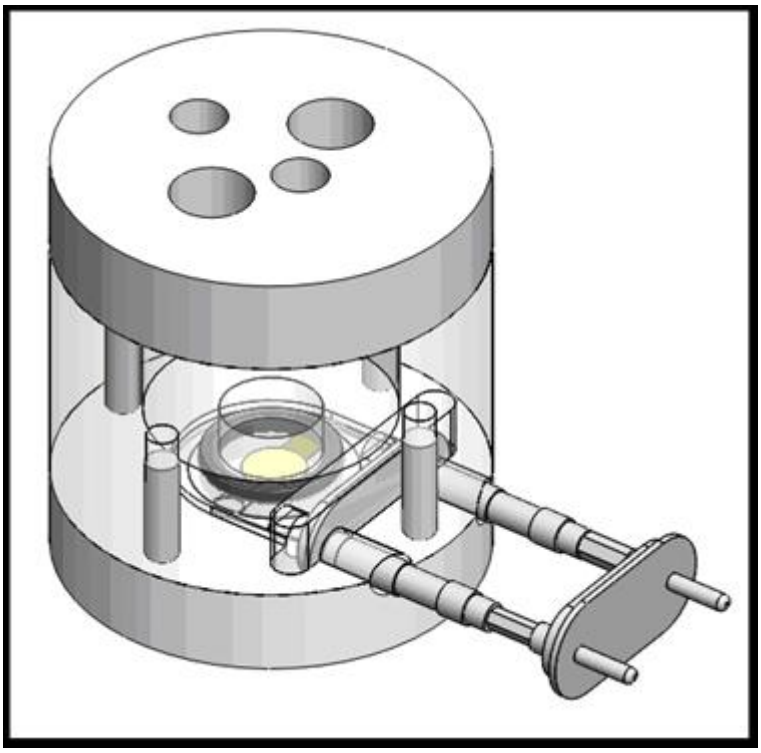

Figure 9 – QCM sensor flow-cell.

4.1.3. Flow Control and Data Acquisition

In order to control the flow-rate of N_2 gas into the experimental setup, the MKS 247C 4-Channel Readout (shown in Figure 10) was utilized with MKS Flo-Controllers (Model # 1479A13CS1AM), shown in Figure 11. A universal counter from Hewlett Packard (Model # 53131A) is photographed in Figure 12, and was used to measure the resonant frequency from QCM sensors in the experiments. The universal counter was connected to a PC via a GPIB connection for data communication. Data acquisition was handled using the LabVIEW program, the graphical user interface (GUI) of which is shown in Figure 13.

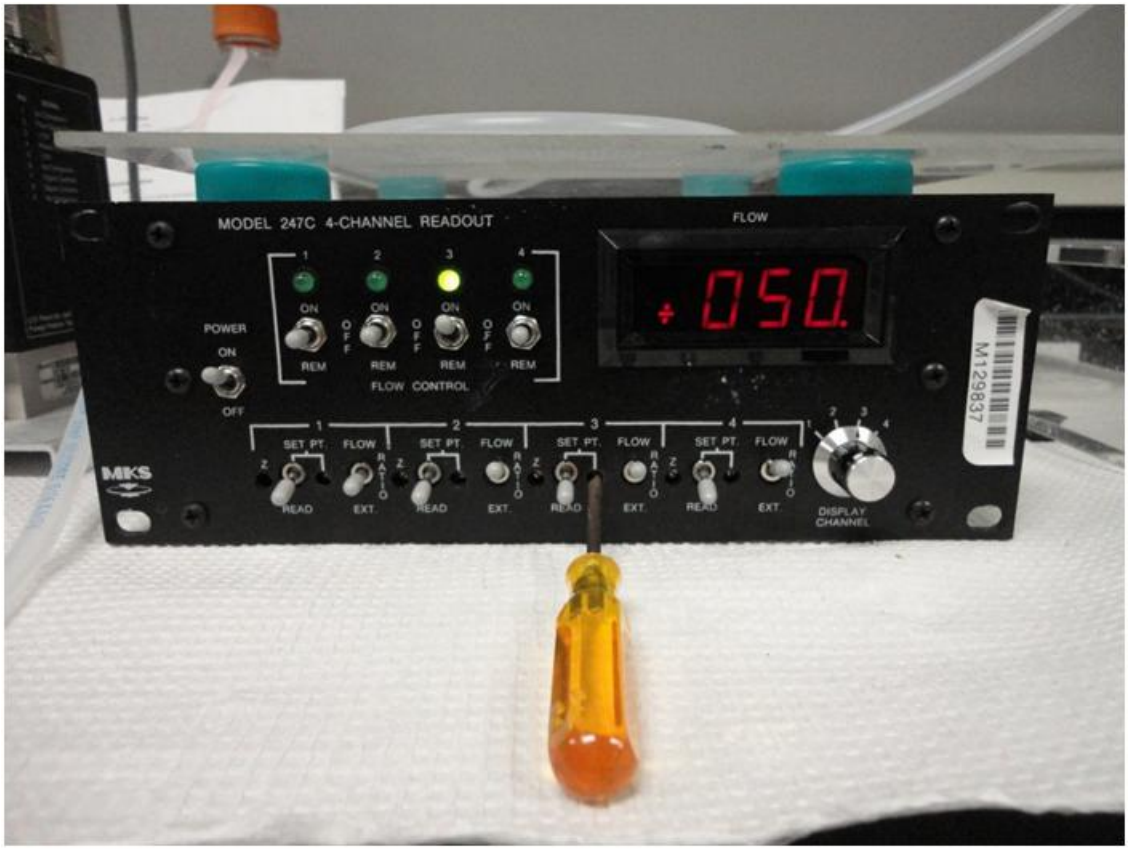

Figure 10 – MKS 247C 4-channel readout.

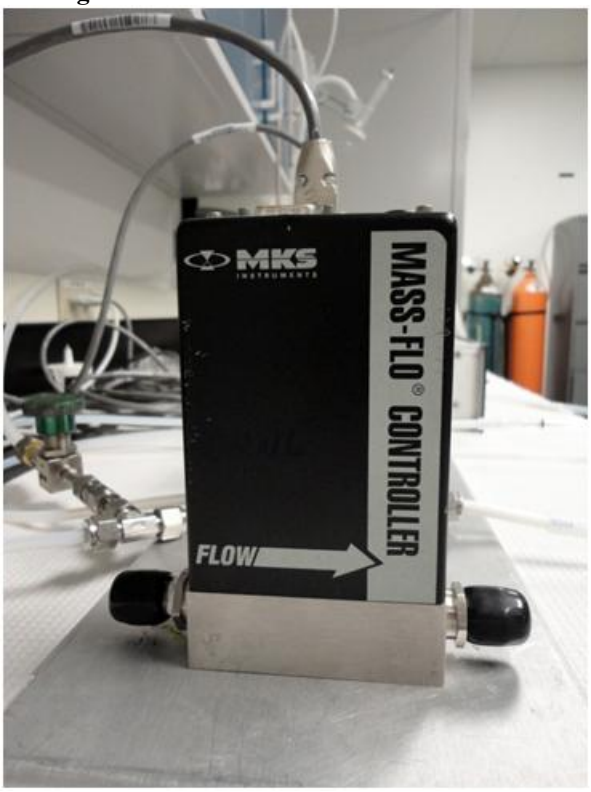

Figure 11 – MKS Flo-Controller.

Figure 12 – Hewlett Packard (HP) 53131A universal counter.

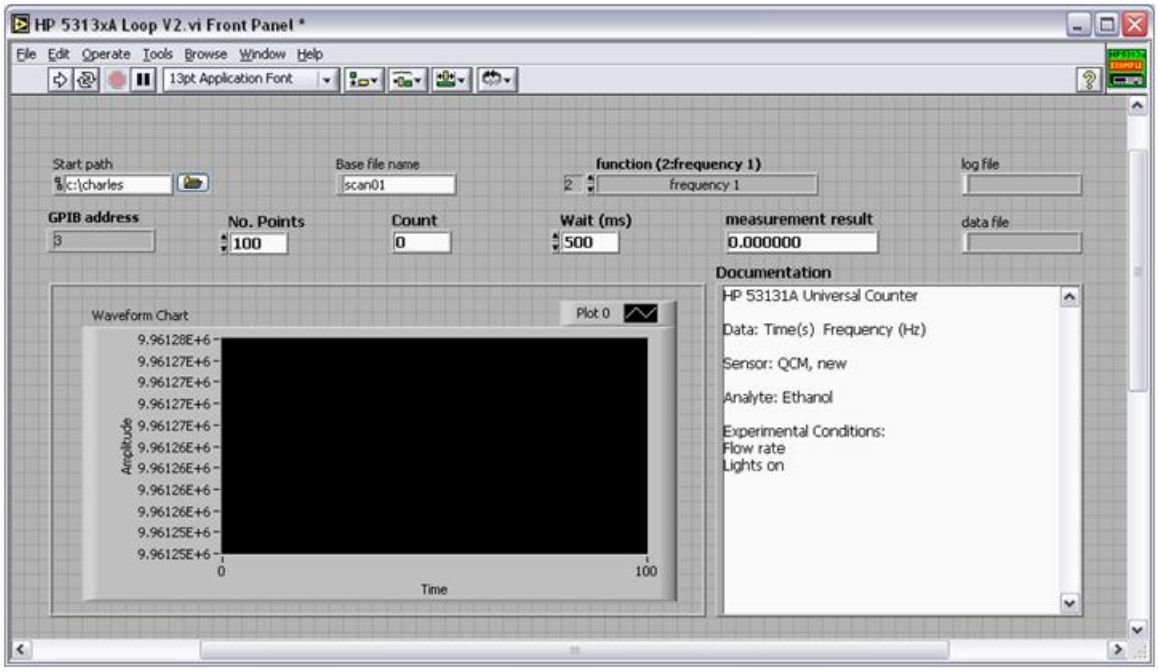

Figure 13 – LabVIEW GUI of MeHg monitor.

4.1.4. Experimental Plan and Procedures

The experimental plan of Stage #1 experiments using both polished and etched surface QCM sensors, and experimenting with flow-rates of 18 and 50 mL/min using a 100 mg/L $HgCl_2$ standard is exhibited in Table 2. The five different concentrations that were tested aided in determining the linearity of the developing method.

The experimental procedure used for polished and etched surface QCM sensor experiments in Stage #1 is conveyed in Tables 3 and 4 respectively. The need for different procedures for the different surfaces of QCM sensors is because etched surface QCM sensors take a greater amount of time in reaching equilibrium. Constant monitoring until equilibrium was needed to ensure that no irregularities in that time interval occurred. The difference in recording times of frequency response data for polished and etched surface QCM sensors was 50 and 240 minutes respectively. The "Count" and "Total Count" columns of Tables 3 and 4 signify the variable utilized in the LabVIEW program for defining the amount of time needed to record. The Count variable was defined as the amount of samples per second where all frequency recordings were sampled at 2 samples/second.

Table 2 – Experimental Plan of Stage #1

mg/L	µg/L	Hg (mg)	100 mg/L Standard (µL)	100 mg/L Standard (mL)
9.05	9050	1	10000	10
4.74	4740	0.5	5000	5
1.95	1950	0.2	2000	2
0.98	9800	0.1	1000	1
0	0	0	0	0
* Performed at 18 and 50 mL/min at room temperature				
** Performed using 100 mg/L standard				
*** Performed for both polished and etched QCM sensors				

Table 3 – Experimental Procedure for Stage #1, Polished Surface QCM Sensors

Step	*Time (min)*	*Total Time (min)*	*Count*	*Total Count*	*Purpose*
0	-	-	-	-	Warm up QCM oscillator chip until obtaining a stable resonant frequency. There is no gas running to the sensor.
1	20	20	2400	2400	Purge bubbler for 20 min at 350 mL/min using nitrogen or argon gas. The bubbler is connected to the gold trap, which is not connected to the QCM sensor.
2	2	22	240	2640	Adjust flow to the gold trap to the needed flow rate and connect the outlet of the gold trap to the QCM sensor.
3	5	27	600	3240	Heat gold trap to 450°C.
4	10	37	1200	4440	Keep gas flow w/o heat on gold trap.
5	13	50	1560	**6000**	Turn gas off and let QCM sensor obtain equilibrium.

Table 4 – Experimental Procedure for Stage #1, Etched Surface QCM Sensors

Step	*Time (min)*	*Total Time (min)*	*Count*	*Total Count*	*Purpose*
0	-	-	-	-	Warm up QCM oscillator chip until obtaining a stable resonant frequency. There is no gas running through the sensor.
1	20	20	2400	2400	Purge bubbler for 20 min at 350 mL/min using nitrogen or argon gas. The bubbler is connected to the gold trap, which is not connected to the QCM sensor.
2	2	22	240	2640	Adjust flow to the gold trap to the needed flow rate and connect the outlet of the gold trap to the QCM sensor.
3	5	27	600	3240	Heat gold trap to 450°C.
4	10	37	1200	4440	Keep gas flow w/o heat on gold trap.
5	203	240	24360	**28000**	Turn gas off and let QCM sensor obtain equilibrium.

4.1.5. Preparation of Standards and Solutions

100 mg/L $HgCl_2$ standard: 100 mg $HgCl_2$ was dissolved in 10% HCl, and transferred to a 1000 ml volumetric flask and the volume is completed with 10% HCl.

20% (w/v) Stannous chloride: 10 ml of HCl (con.) were added to 20 g of $SnCl_2.2H_2O$ and the volume is then completed up to 100 ml using DI water. The $SnCl_2$ solution was then purged with N_2 gas overnight at 350 mL/min.

4.1.6. Preparation of Experimental Glassware

All glassware used throughout these experiments were cleaned by first rinsing with DI water, filling them with 30% HCl solution, and letting them sit overnight. The next day, the glassware was rinsed with 1% HCl solution and rinsed again with DI water. This was to ensure that any inorganic Hg was eliminated from the glassware before using for experimentation.

4.2 Stage #2 Experiment

Stage #2 is shown in Figure 14 where the concentration of organic Hg (e.g. MeHg) was measured. This was accomplished with the use of aqueous phenylation, which used $NaBPh_4$ as the derivatization reagent. The derivative formed (e.g. MeHgPh) was purged from the solution in the bubbler (heated to $50^{O}C$) using N_2 gas at 200 mL/min for 45 min and trapped on the Tenax trap. The MeHgPh was released from the trap by heating to $250^{O}C$. MeHgPh vapor then traveled to the pyrolysis coil which was heated to $800^{O}C$ in order to convert MeHgPh to Hg^0. The Hg^0 vapor was then sent to the flow cell at 18 mL/min where an etched surface QCM sensor was utilized for sensing. The flow-rate and

etched surface QCM sensor were used based on results generated from the Stage #1 experiment. The reasoning behind these decisions will be further discussed in Section 5. Different concentrations of MeHg were utilized to determine the feasibility of the instrument.

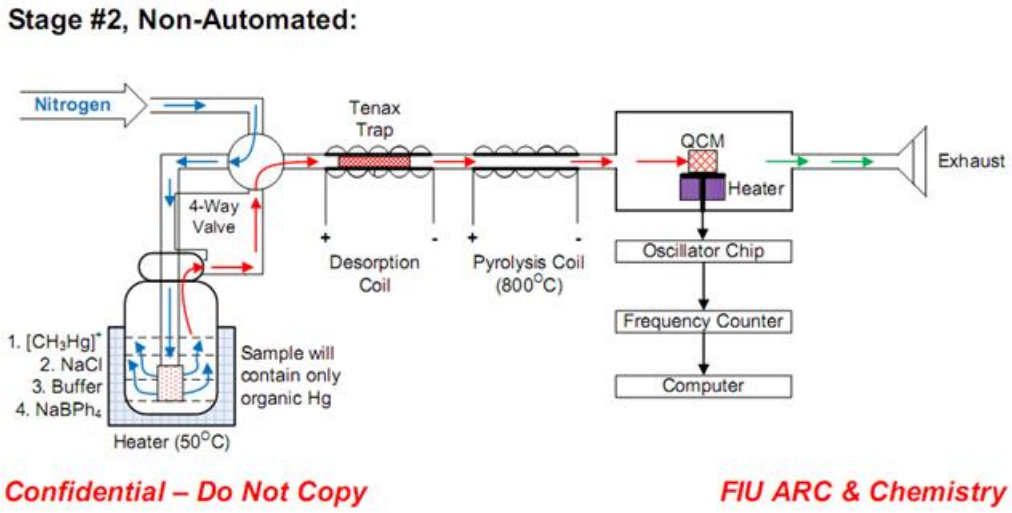

Figure 14 – Stage #2 of MeHg experimental plan.

4.2.1. Derivatization of MeHg using Aqueous Phenylation

The experimental setup of the derivatization and P&T method for Stage #2 is shown in Figure 15 which used aqueous phenylation [88] to derive organic Hg from the solution. This was accomplished by mixing 100 mL of 30% sodium chloride (NaCl) solution, 2 mL of citric buffer solution, 1 mL of $NaBPh_4$, and 1 mg/L MeHg standard needed for the experiment in a 200 mL bubbler. The bubbler was then soaked in a hot water bath (shown in Figure 16) at 50°C for 5 minutes in order to increase volatility. The solution was then purged at 200 mL/min in the same hot water bath with N_2 gas for 45 minutes into a Tenax trap shown in Figure 17. The gold trap was then heated to 250°C for 5 minutes using a heating coil connected to a variable voltage controller. During this time, N_2 gas was flowing at 18 mL/min to transport the organic Hg being released by the Tenax trap to the QCM sensor.

Figure 15 – Experimental setup of Stage #2 (Chemical Separation).

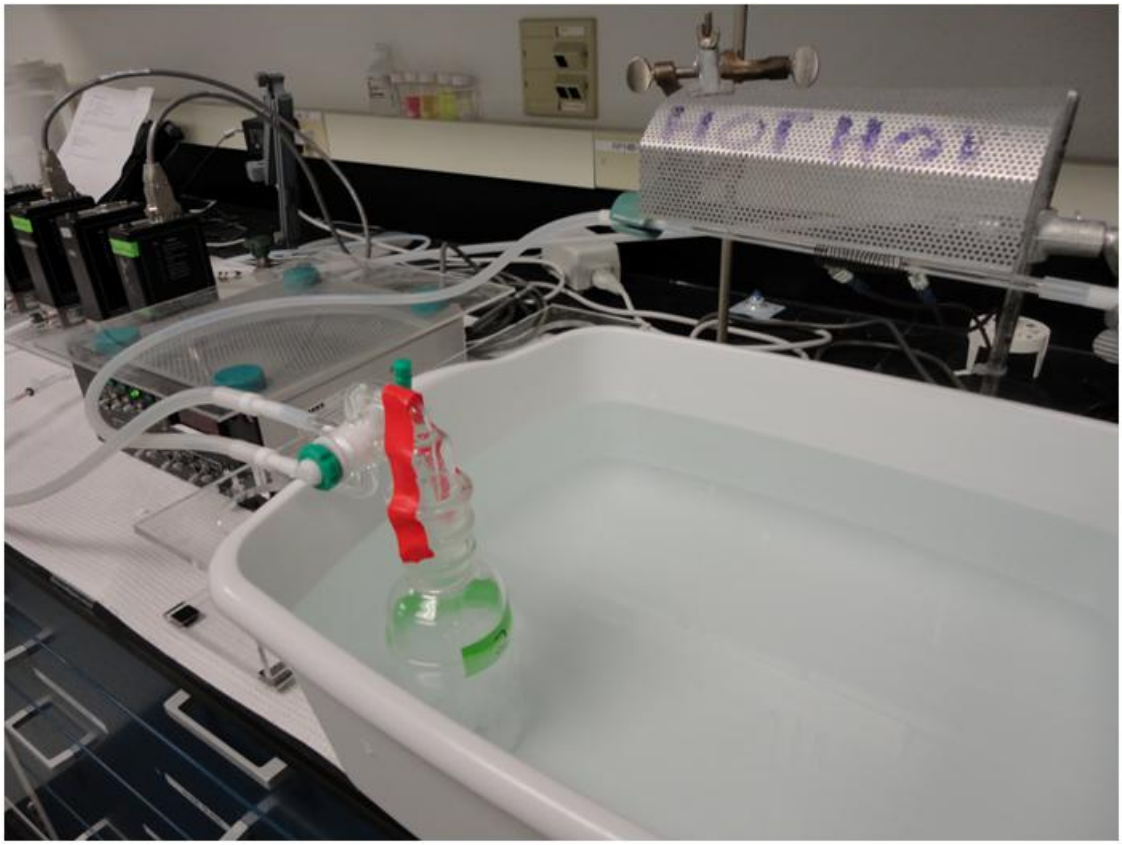

Figure 16 – Hot water bath at ≈45°C for aqueous phenylation.

Figure 17 – Tenax trap in P&T method.

4.2.2. Sensing using QCM Sensors

The experimental setup of the sensing aspect of this project was the same setup used for Stage #1 (presented in Figure 7).

4.2.3. Flow Control and Data Acquisition

The flow control and data acquisition utilized was the same equipment as Stage #1.

4.2.4. Experimental Plan and Procedures

The experimental plan of Stage #2 experiments using etched surface QCM sensors and the experiments with a flow-rate of 18 mL/min using a 1 mg/L MeHg standard are exhibited in Table 5. The experimental procedure used for etched surface QCM sensor experiments in Stage #2 is conveyed in Table 6.

Table 5 – Experimental Plan of Stage #2

ppm	*ppb*	*Hg (mg)*	*1 ppm Standard (mL)*
0	0	0	0
0.001	1	0.0001	0.1
0.005	5	0.0005	0.5
0.01	10	0.001	1
0.015	15	0.0015	1.5
* Performed at 18 mL/min at room temperature			
** Performed using 1 ppm standard			
*** Performed for etched QCM sensor			

Table 6 – Experimental Procedure for Stage #2

Step	*Time (min)*	*Total Time (min)*	*Count*	*Total Count*	*Purpose*
0	-	-	-	-	Warm up QCM oscillator chip until obtaining a stable resonant frequency. There is no gas running through the sensor.
1	15	15	-	-	Mix all of the reagents into bubbler in order to react. There is no gas running through the sensor.
2	45	60	-	-	Purge bubbler for 45 min at 200 mL/min using nitrogen or argon gas. The bubbler is connected to the Tenax trap which is not connected to the QCM sensor.
3	10	70	1200	1200	Heat Tenax trap to 250°C. The Tenax trap is connected to the Pyrolysis coil which is heated at 800 degrees Celsius. The Pyrolysis coil is connected to the QCM sensor. Gas flow is set to 18 mL/min.
4	10	80	1200	2400	Keep gas flow w/o heat on Tenax trap and Pyrolysis coil.
5	220	300	26400	**28800**	Turn gas off and let QCM sensor obtain equilibrium.

4.2.5. Preparation of Standards and Solutions

30% NaCl solution: 600 g of NaCl is dissolved in DI water and the volume is then completed up to 2000 mL using DI water.

Citric buffer solution: 43.05 g of citric acid ($C_6H_8O_7$) and 86.73 g of sodium citrate ($C_6H_5Na_3O_7 \cdot 2H_2O$) are dissolved in DI water and the volume is then completed up to 500ml using DI water.

1% $NaBPh_4$: 1 g of $NaBPh_4$ is dissolved in DI water and the volume is then completed up to 100ml using DI water.

0.2 M Potassium Bromide (KBr): 11.900 g of KBr (certified ACS grade) are heated overnight in a glass scintillation vial (Kimble 74511) at 250°C +/- 20°C in a furnace to remove HG. After cooling, the KBr is dissolved in 500 mL of DI water and stored in a borosilicate bottle. It is prepared on a weekly basis.

0.1 M Potassium Bromate ($KBrO_3$): 8.385 g of $KBrO_3$ (certified ACS grade) are heated overnight in a glass scintillation vial (Kimble 74511) at 250°C +/- 20°C in a furnace to remove Hg. After cooling, the $KBrO_3$ is dissolved in 500 mL of DI water and stored in a borosilicate bottle. It is prepared on a weekly basis.

Mixed brominating reagent (0.1 M Potassium bromide (KBr) and 0.05 M Potassium bromate (KBrO3)): Equal volumes (100 mL) of $KBrO_3$ and KBr solutions are mixed in a 250 borosilicate bottle with a Teflon cap. It is prepared on a weekly basis.

4.2.6. Preparation of Experimental Glassware

All glassware used throughout these experiments were cleaned by first rinsing with DI water, then filling the glassware with DI water, 1% of HCl, and 2% of bromide reagent. This solution then sat in the glassware overnight. The following day, the glassware was soaked with 30% HCl solution, and sat again overnight. The next day, the glassware was rinsed with 1% HCl solution and rinsed again with DI water. This ensured that any inorganic and organic Hg was eliminated from the glassware before using for experimentation.

4.3 QCM Sensor Regeneration

Sensor regeneration was accomplished by following the procedure shown in Table 7. The QCM sensor was heated to 150°C [83][90][91] to desorb Hg from the sensor's surface.

Table 7 – QCM Sensor Regeneration Procedure

Step	*Time (min)*	*Total Time (min)*	*Count*	*Total Count*	*Purpose*
1	5	5	600	600	Heat QCM sensor to 150°C with a flow of N_2 gas at 50 mL/min.
2	5	10	600	1200	Continue with N_2 gas flow at 50 mL/min.
3	470	480	56400	**57600**	Monitor resulting frequencies.
* Gas is connected directly to the QCM sensor.					

5. RESULTS AND ANALYSIS

The results and analysis of the project will now be discussed and includes Stage #1, Stage #2, and QCM regeneration. Stage #1 dealt with the measurement of inorganic Hg using EPA's Method 1631 Revision E. Both polished and etched surface QCM sensors were experimented with at 18 and 50 mL/min. Stage #2 dealt with the measurement of organic Hg using aqueous phenylation. Based on the results of Stage #1, etched surface QCM sensors were utilized at 18 mL/min, which gave the highest frequency. The behavior of polished and etched QCM sensors during regeneration was also examined through frequency response and observance using microscopy.

5.1 Stage #1 Experiments

Table 8 presents the frequency shift of the various Hg concentrations shown in Table 2 for polished surface QCM sensors at 18 mL/min. Figures 34 through 38**Error! Reference source not found.** in Appendix B shows the frequency responses and Figure 18 are the cumulative frequency shifts at 18 mL/min. Figure 19 presents a calibration curve with a good gradient using data represented in Table 8.

Table 8 – Frequency Shifts of Polished Surface QCM Sensor at 18 mL/min

Conc. (mg/L)	*ΔF (Hz)*
0	7
1	3
2	6
5	14
10	26

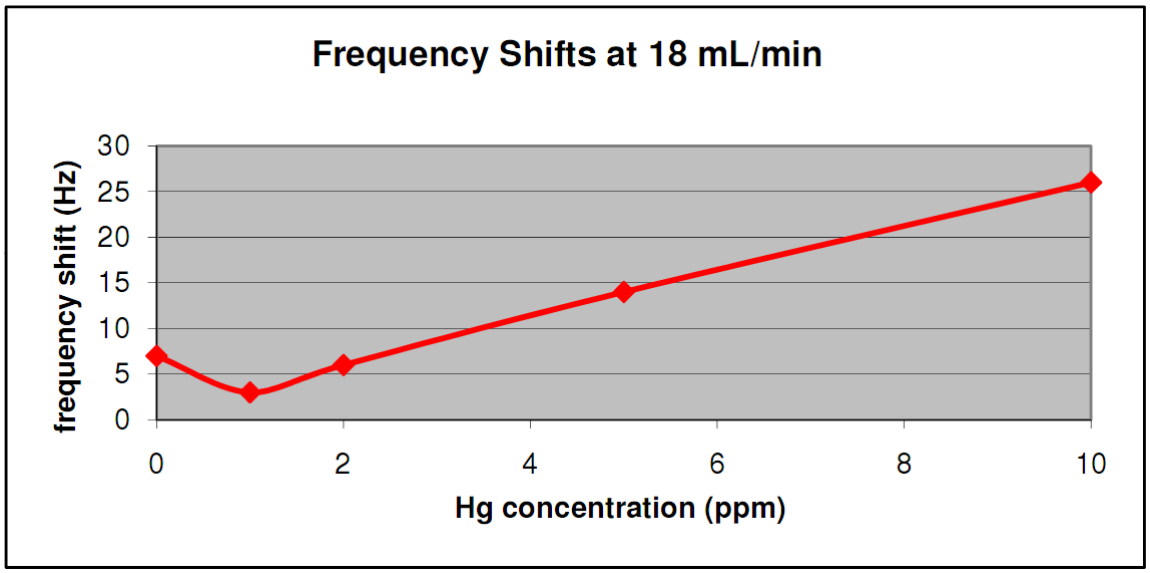

Figure 18 – Graph of frequency shifts of polished surface QCM sensor at 18 mL/min (Stage #1).

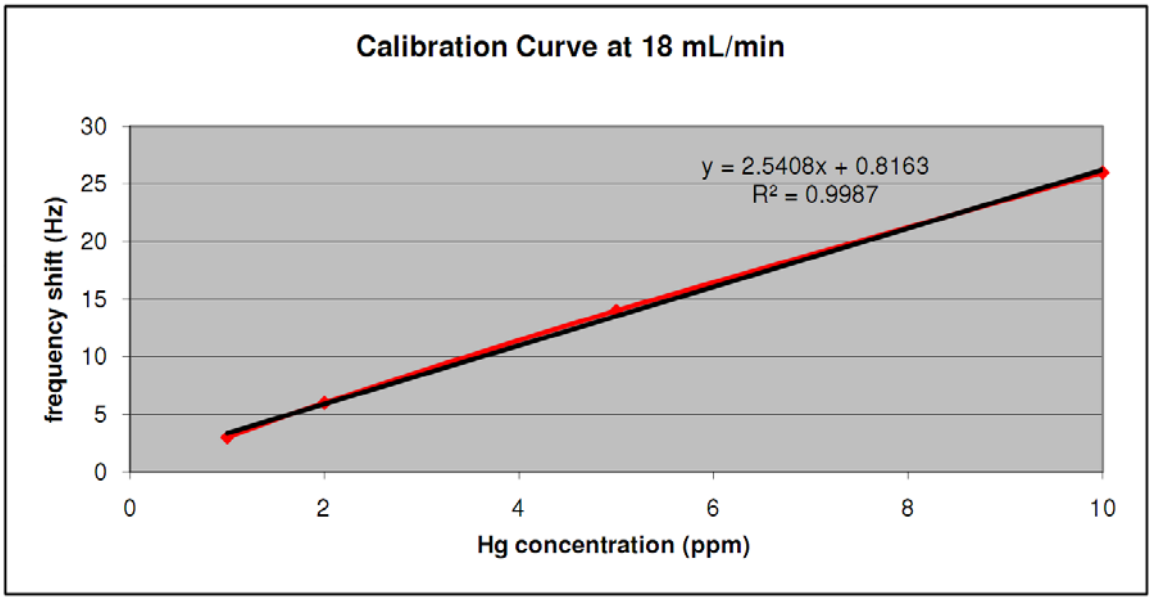

Figure 19 – Calibration curve for polished surface QCM sensor at 18 mL/min (Stage #1).

Table 9 depicts the frequency shifts of each Hg concentration that was studied in Table 2 for polished surface QCM sensors at 50 mL/min. The Hg concentrations and frequency shifts in red did not correlate well with other cases in the experimentation which were found through determining the gradient. The calibration curve is shown in Figure 21 with the R^2 value being 0.957. Figures 39 through 43 show the frequency responses of each Hg concentration shown in Table 2, and Figure 20 displays the trend of those frequency responses.

Table 9 – Frequency Shifts of Polished Surface QCM Sensor at 50 mL/min

Conc. (mg/L)	*ΔF (Hz)*
0	4
1	10
2	16
5	50
10	73

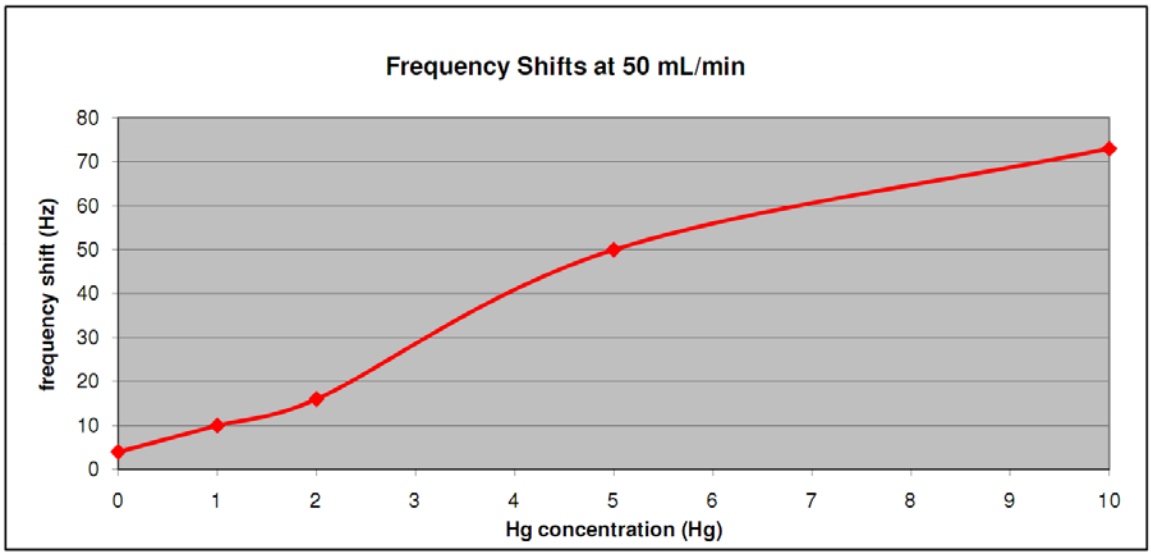

Figure 20 – Graph of frequency shifts of polished surface QCM sensor at 50 mL/min (Stage #1).

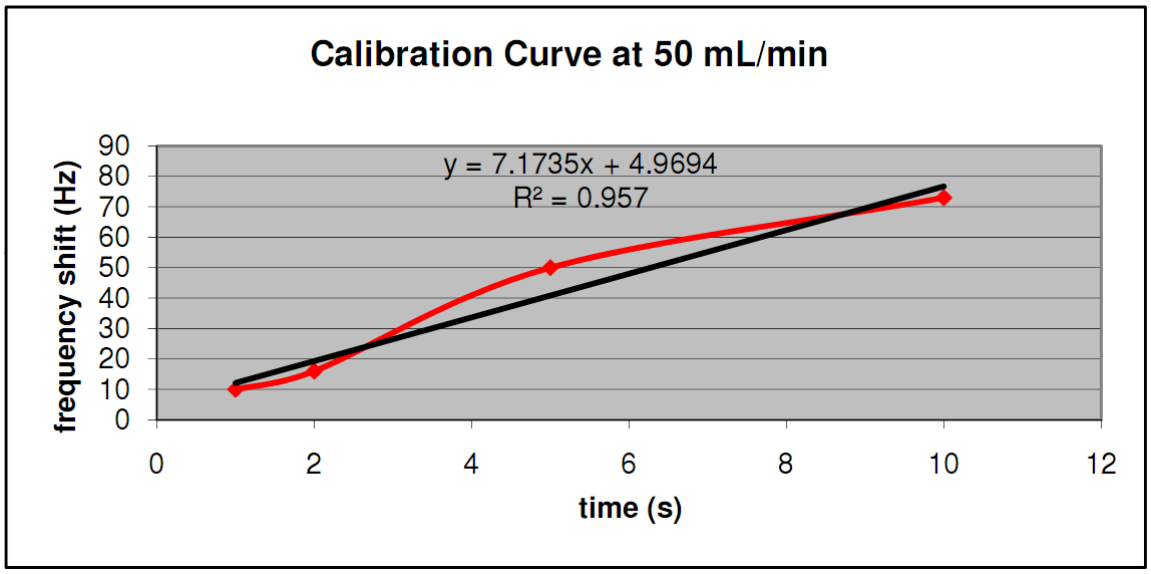

Figure 21 – Calibration curve for polished surface QCM sensor at 50 mL/min (Stage #1).

Table 10 shows the different frequency shifts of each of the concentrations in Table 2 for etched surface QCM sensors at 18 mL/min. Figures 44 through 48 presents the frequency response of each experiment shown in Table 2, Figure 22 is the trend of the frequency shifts, and Figure 23 shows the calibration curve with six points having a R^2 value of 0.9888.

Table 10 – Frequency Shifts of Etched Surface QCM Sensor at 18 mL/min

Conc. (ppb)	*ΔF (Hz)*
0	-14
1	20
2	83
5	170
10	421

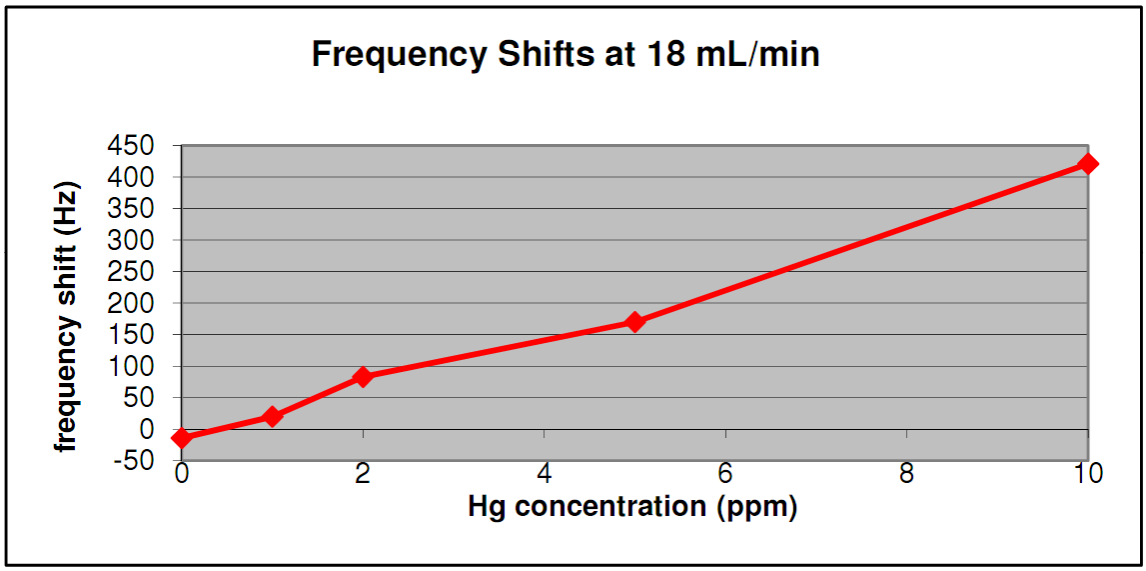

Figure 22 – Graph of frequency shifts of etched surface QCM sensor at 18 mL/min (Stage #1).

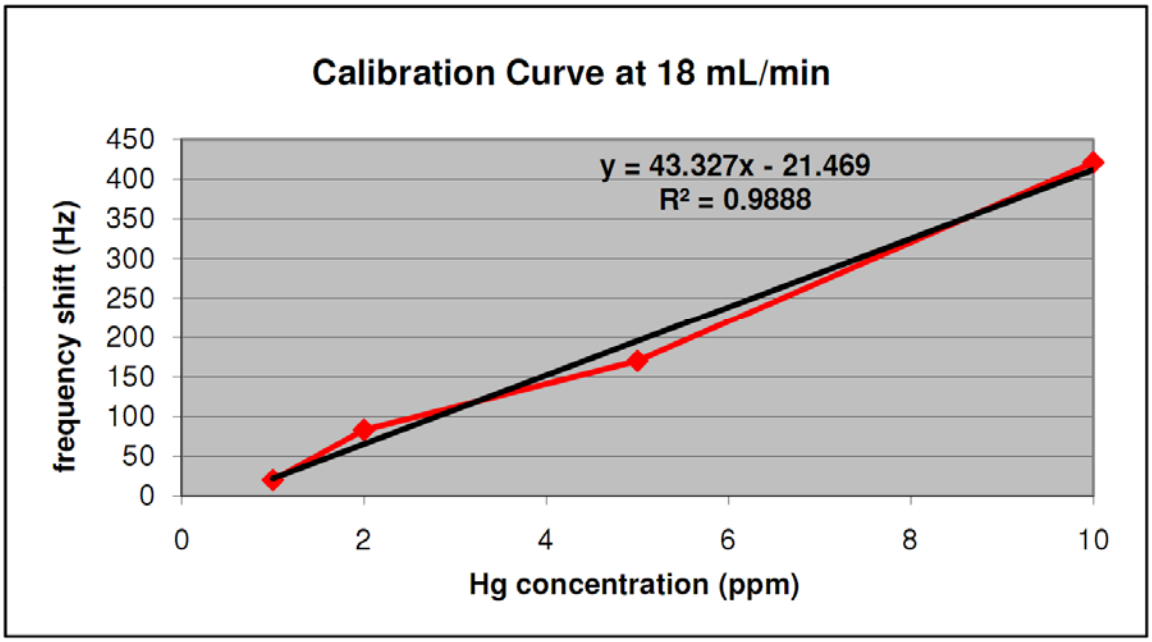

Figure 23 – Calibration curve for etched surface QCM sensor at 18 mL/min (Stage #1).

Table 11 depicts the frequency shifts of each Hg concentration shown in Table 2 for etched surface QCM sensors at 50 mL/min. The calibration curve is shown in Figure 25 where the R^2 value is 0.9864. Figures 49 through 53 show the frequency responses of each Hg concentration in Table 2 and Figure 24 displays the trend of those frequency responses.

Table 11 – Frequency Shifts of Etched Surface QCM Sensor at 50 mL/min

Conc. (ppm)	*ΔF (Hz)*
0	-4
1	6
2	27
5	40
10	85

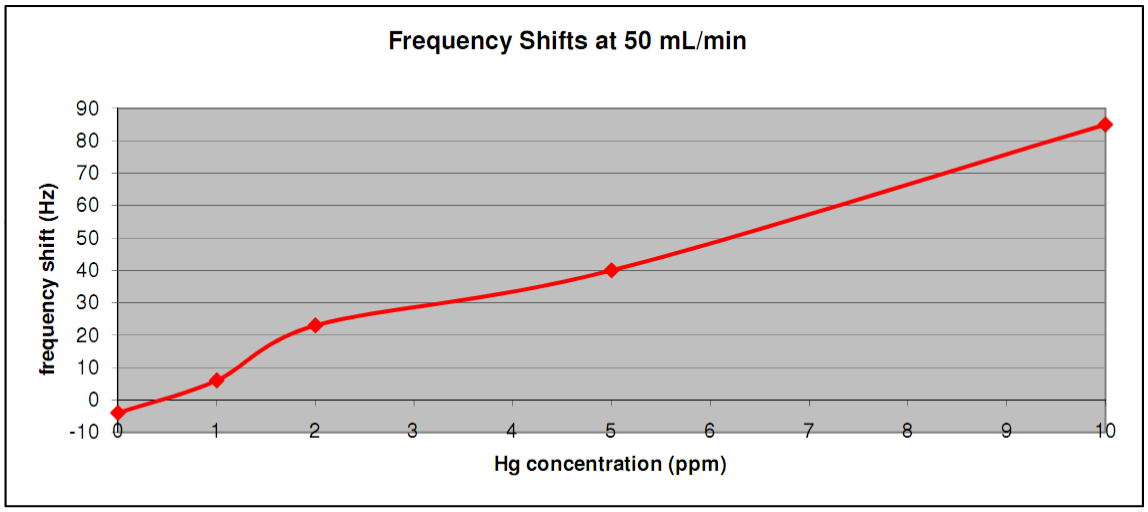

Figure 24 – Frequency shifts at 50 mL/min flow rate (Stage #1).

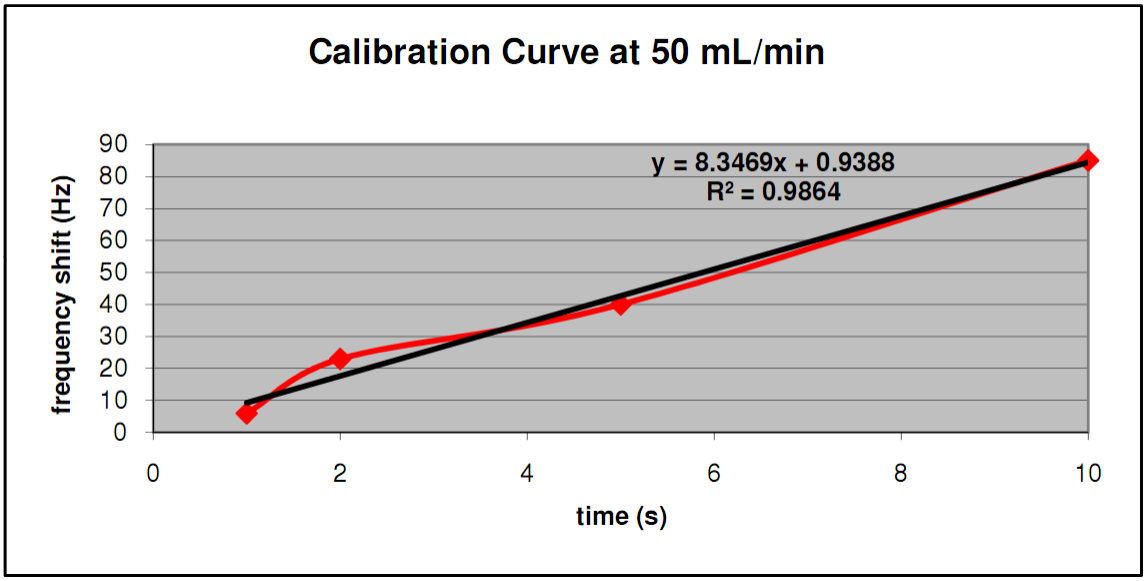

Figure 25 – Calibration curve at 50 mL/min flow rate (Stage #1).

5.2 Stage #2 Experiments

Table 12 shows the different frequency shifts of each of the concentrations exhibited in Table 5. The resulting frequency shifts for all concentrations were well below the needed responses. This is due to the µg/L concentrations that were studied. Future studies are needed in the range of 1 mg/L to 10 mg/L concentrations using organic Hg to receive adequate frequency responses which correspond to results from Stage #1 experiments. Figures 54 through 60 present the frequency response of each experiment shown in Table 5.

Table 12 – Frequency Shifts for Stage #2

Conc. (ppb)	*ΔF (Hz)*
0	15
1	11
2	1
5	4
10	8
15	14
17	16

5.3 QCM Regeneration

Regeneration of a polished (ID# 8P) and etched (ID# 1E) surface QCM sensors is shown in Figures 26 and 27 respectively. The expected reaction of the procedure presented in Table 7 was an increase in the resonant frequency once Hg was desorbed. The opposite occurred however, where the resonant frequency decreased by 5,111 Hz and 5,161 Hz for polished and etched QCM sensors respectively. Images taken from an x10 microscope (Nikon 1002908 with Pixelink camera) showed that Hg was successfully desorbed. These images are shown in Figures 28 through 33.

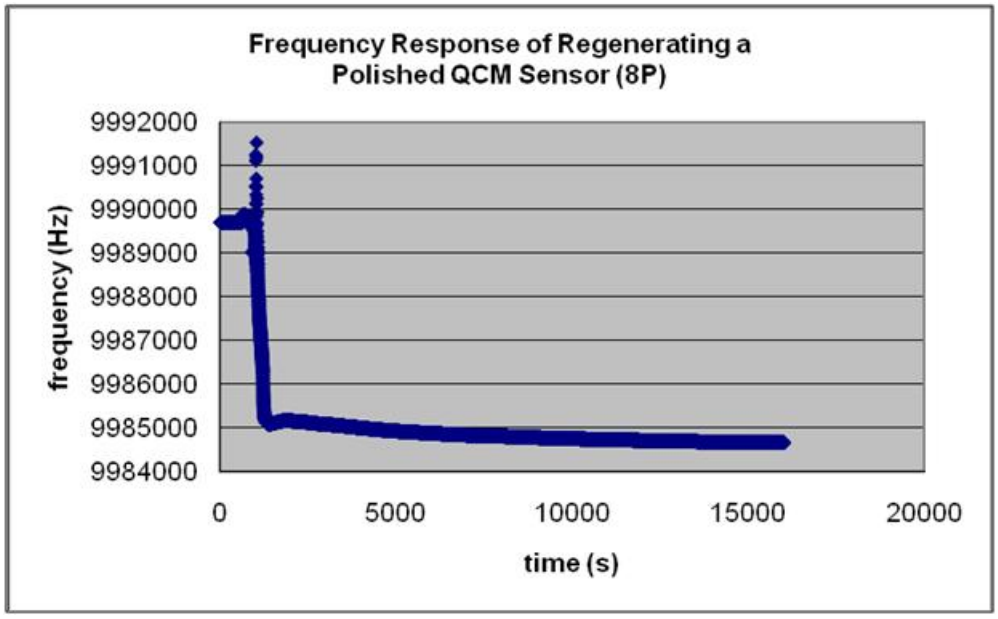

Figure 26 – Frequency response of regenerating a polished QCM sensor.

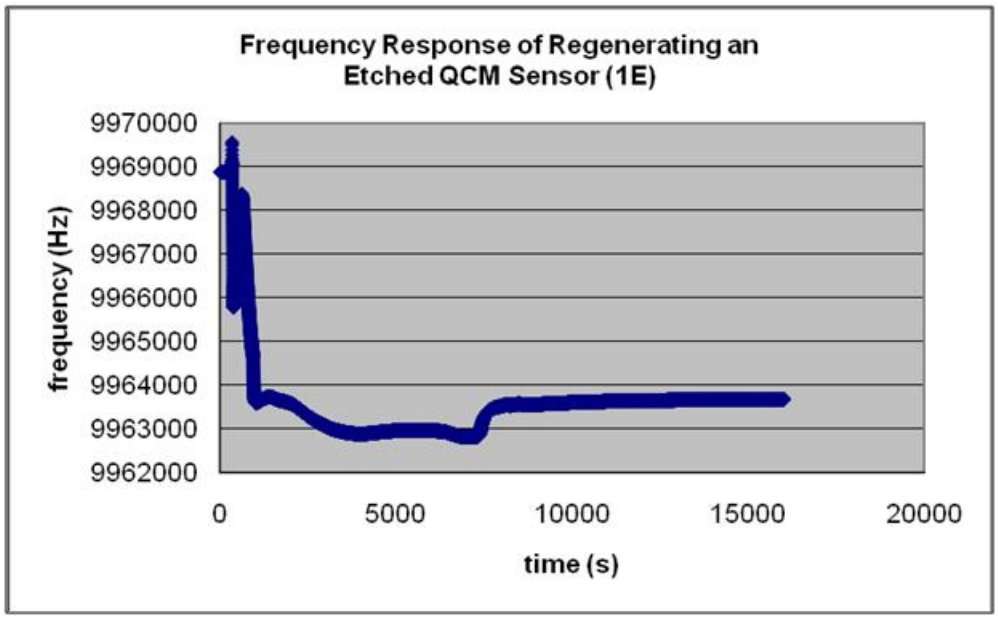

Figure 27 – Frequency response of regenerating an etched QCM sensor.

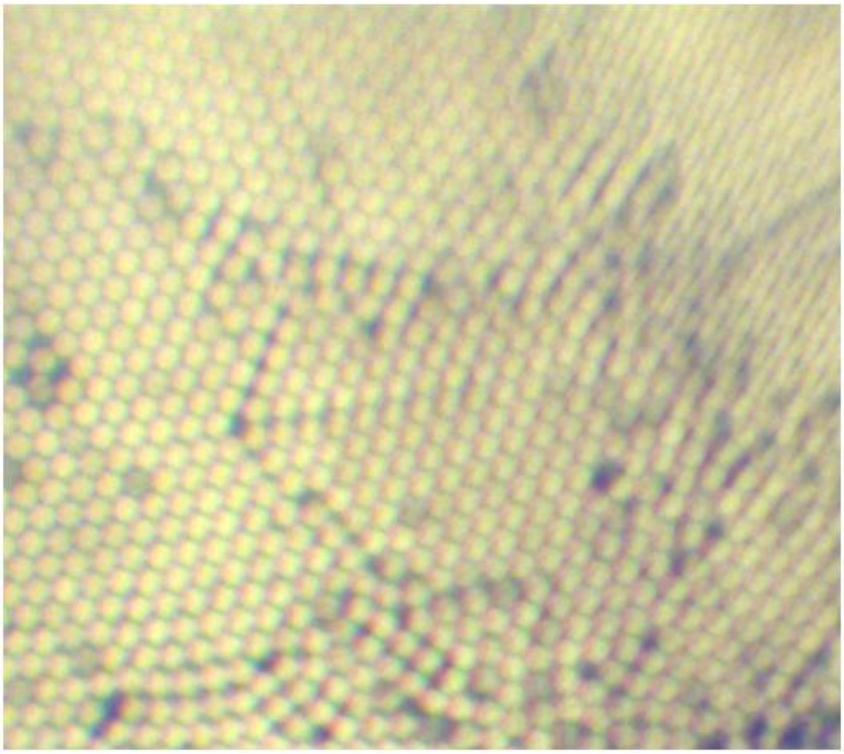

Figure 28 – New polished QCM sensor (9P).

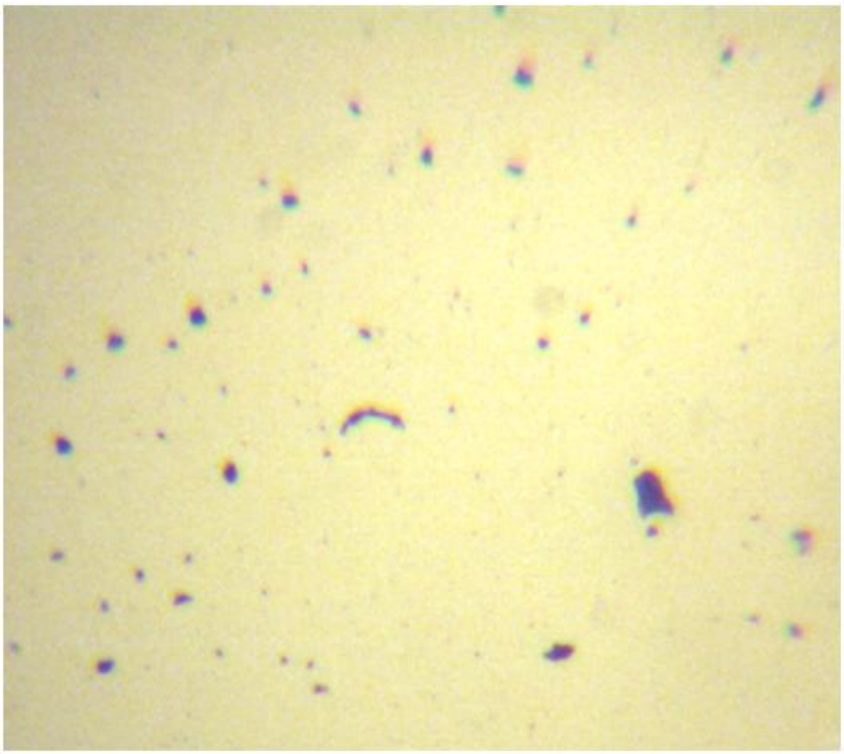

Figure 29 – Used polished QCM sensor (8P).

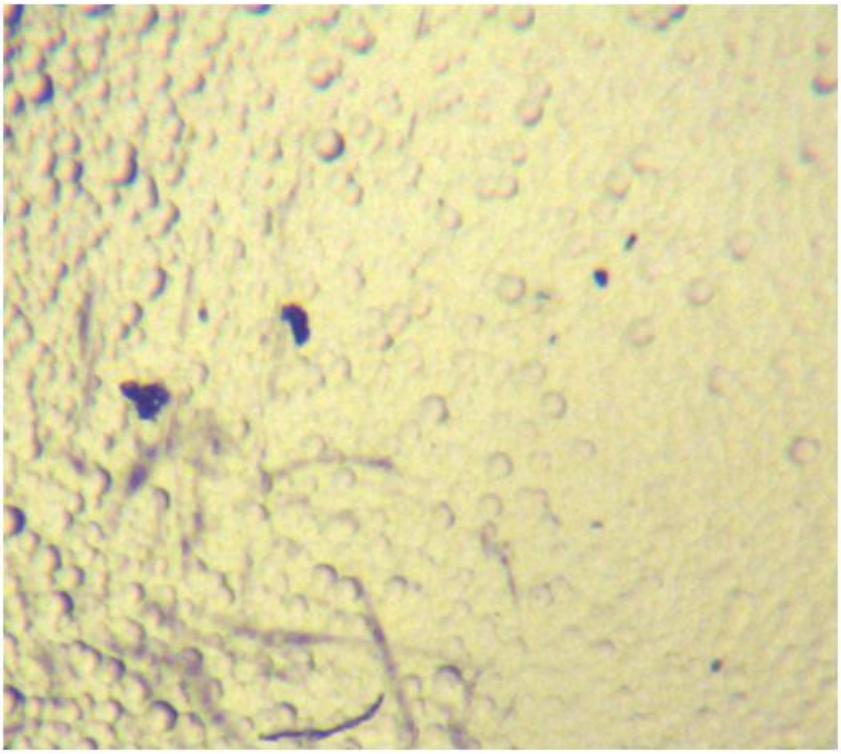

Figure 30 – Regenerated polished QCM sensor (8P).

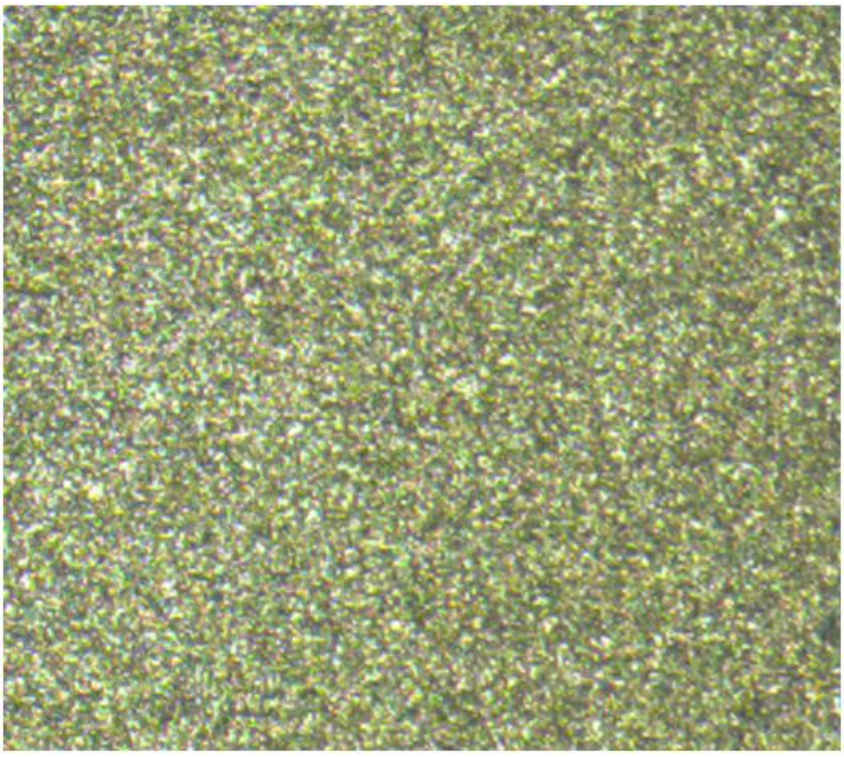

Figure 31 – New etched QCM sensor (2E).

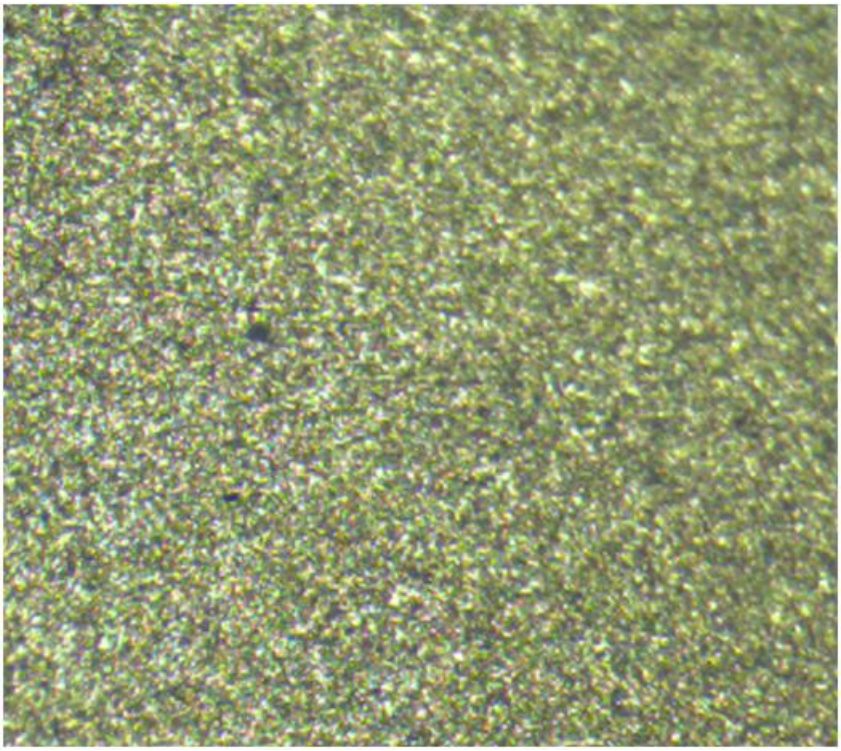

Figure 32 – Used etched QCM sensor (1E).

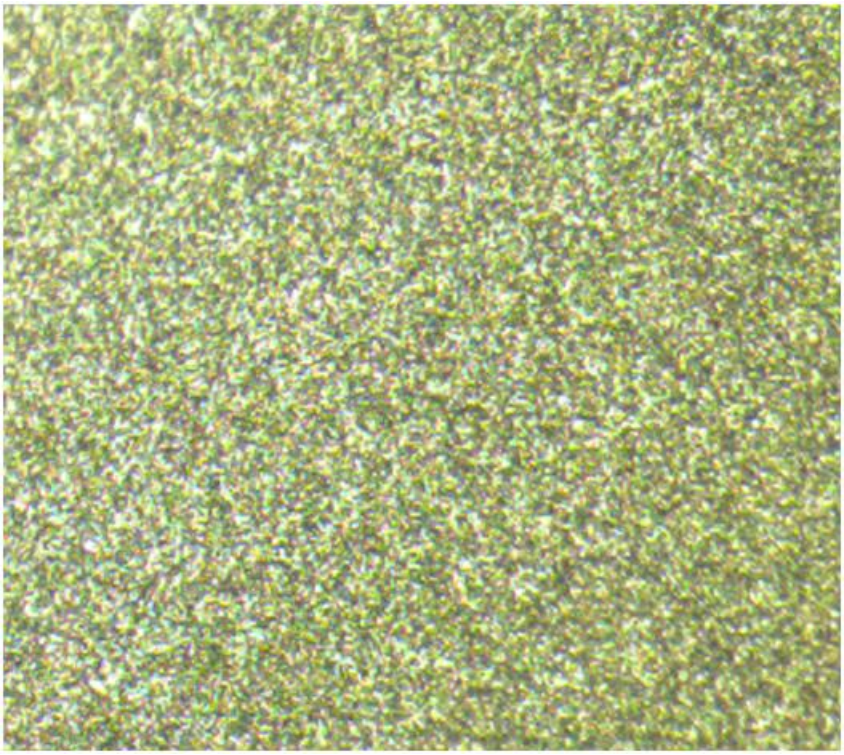

Figure 33 – Regenerated etched QCM sensor (1E).

6. CONCLUSION

The focus of this project was a proof-of-concept using chemical derivatization, the P&T method, and QCM sensors in order to measure the amount of Hg (e.g. inorganic and organic) in pore water samples at ORR creek beds. Experiments were performed using both polished and etched surface QCM sensors for inorganic Hg determination at different flow rates (e.g. 18 and 50 mL/min). The variation that produced the best results was then utilized for organic Hg detection, which used etched surface QCM sensors at 18 mL/min. This was due to the high sensitivity given for etched surface QCM sensors at 18 mL/min at various inorganic Hg concentrations during Stage #1 experiments. QCM sensor regeneration was also investigated for both polished and etched surface QCM sensors. Adsorbed Hg on the sensor's surfaces was removed by heating to 150°C. This was validated through microscopy.

Research results generated in this project depict a successful proof-of-concept which uses a chemical derivatization, the P&T method, and QCM sensors. The argument can be made, however, that the resulting mg/L range of detection is far below what is required for the detection of MeHg in environmental samples, which is in the ng/L range. Another issue was that the experimental setup using QCM sensors took far too long to reach equilibrium after injecting Hg into the flow cell. Future work is needed to resolve these issues. This, however, was a good step as it determined whether these different techniques could be successfully integrated. Another step for future research would be to integrate the inorganic and organic Hg detection into experiments currently being planned. Afterwards, other sensing mechanisms such as microcantilever sensors, must be incorporated into this research to receive better lower ranges of detection that can one day be utilized to quickly detect ng/L levels of MeHg in environmental samples.

7. REFERENCES

[1] K. Schambach, K. Eden, K. Schumacher, and G. Wiegleb, "Micromachined Mercury Sensor," *Proceedings of the 30th European Solid-State Device Research Conference (ESSDERC'02)*, pp. 443-446, 2002.

[2] J.J. Caron, R.B. Haskell, D.G. Libby, C.J. Freeman, and J.F. Vetelino, "A surface acoustic wave mercury vapor sensor," *Proceedings of the IEEE International Frequency Control Symposium*, 1997.

[3] S. He, D. Li, C. Zhu, S. Song, L. Wang, Y. Long, and C. Fan, "Design of a gold nanoprobe for rapid and portable mercury detection with the naked eye," *Chemical Communications*, pp. 4885-4887, 2008.

[4] Science Applications International Corporation, *Field Measurement Technology for Mercury in Soil and Sediment: NITRON's XLi/XLt 700 Series X-Ray Fluorescence Analyzers*, Idaho Falls, ID, May 2004.

[5] Science Applications International Corporation, *Milestone Inc.'s Direct Mercury Analyzer (DMA)-80*, Idaho Falls, ID, May 2004.

[6] U.S. Department of Energy (DOE), "2007 Oak Ridge Reservation Annual Site Environmental Report," Internet document, http://www.ornl.gov/sci/env_rpt/aser2007/ aser2007.htm.

[7] F.X. Han, Y. Su, D.L. Monts, C.A. Waggoner, and M.J. Plodinec, "Binding, distribution, and plant uptake of mercury in a soil from Oak Ridge, Tennessee, USA," *Science of the Total Environment*, vol. 368, pp. 753-768, 2006.

[8] E. Philips, "Upper East Fork Poplar Creek watershed," *Oak Ridge, TN: US Department of Energy Mercury Workshop*, November 2004.

[9] T.L. Ashwood, C.R. Olsen, I.L. Larsen, and P.D. Lowry, "Sediment contamination in streams surrounding the Oak Ridge gaseous diffusion plant," *Oak Ridge, TN: Oak Ridge National Laboratory*, 1986.

[10] U.S. Environmental Protection Agency (EPA), "Mercury," Internet document, http://www.epa.gov/mercury/.

[11] U.S. Environmental Protection Agency (EPA), "Wastes – Partnerships – Product Stewardship," Internet document, http://www.epa.gov/epawaste/partnerships/ stewardship/index.htm.

[12] C. McNaughton, "Mercury concentrations in fish: implications of Dissolved Organic Matter (DOM) on methylation rates in aquatic systems," Internet document, http://www.deq.utah.gov/Issues/Mercury/prior_meetings.htm.

[13] D.P. Krabbenhoft and D.A. Rickert, "Mercury contamination of aquatic ecosystems," *U.S. Geological Survey*, June 12, 2003.

[14] N.L. Bella and A. Hilliker, "Mercury in the environment," *The Traprock*, vol. 2, pp. 33-36, December 2003.

[15] A. Childress, "Mercury Cycle," *Purdue Research Foundation*, Internet document, http://pasture.ecn.purdue.edu/~mercury/src/cycle.htm.

[16] National Aeronautics and Space Administration, "Aquatic Mercury Cycle," Internet document, http://daac.gsfc.nasa.gov/oceancolor/locus/images/aq_mercury.jpg.

[17] S.M. Ullrich, T.W. Tanton, and S.A. Abdrashitova, "Mercury in the aquatic environment: a review of factors affecting methylation," *Critical Reviews in Environmental Science and Technology*, vol. 35, no. 5, pp. 241-293, 2005.

[18] H. Hintelmann, K. Keppel-Jones, and R.D. Evans, "Constants of mercury methylation and demethylation rates in sediments and comparison of tracer and ambient mercury availability," *Environmental Toxicology and Chemistry Journal*, vol. 19, pp. 2204-2211, 2000.

[19] J.M. Bubb, T.P. Williams, and J.N. Lester, "The behavior of mercury within a contaminated tidal river system," *Water, Science, and Technology Journal*, vol. 28, pp. 329, 1993.

[20] S.M. Callister and M.R. Winfrey, "Microbial methylation of mercury in upper Wisconsin River sediments," *Water, Air, and Soil Pollution Journal*, vol. 29, pp. 453, 1986.

[21] R.A. Bodaly, J.W.M. Rudd, R.J.P. Fudge, and C.A. Kelly, "Mercury concentrations in fish related to size of remote Canadian Shield lakes," *Canadian Journal of Fisheries and Aquatic Sciences*, vol. 50, pp. 980, 1993.

[22] P.S. Ramlal, C.A. Kelly, J.W.M. Rudd, and A. Furutani, "Sites of methyl mercury production in remote Canadian Shield lakes," *Canadian Journal of Fisheries and Aquatic Sciences*, vol. 50, pp. 980, 1993.

[23] J.J. Akielaszek and T.A. Haines, "Mercury in the muscle-tissue of fish from 3 Northern Maine lakes," *Bulletin of Environmental Contamination and Toxicology*, vol. 27, pp. 201, 1981.

[24] W.A. Scheider, D.S. Jeffries, and P.J. Dillon, "Effects of acidic precipitation on Precambrian freshwaters in southern Ontario," *Journal of Great Lakes Research*, vol. 5, pp. 45, 1979.

[25] T. Matilainen, M. Verta, M. Niemi, and A. Uusirauva, "Specific rates of net methylmercury production in lake sediments," *Water, Air, and Soil Pollution Journal*, vol. 56, pp. 595, 1991.

[26] J.J. Bisogni and A.W. Lawrence, "Kinetics of mercury methylation in aerobic and anaerobic aquatic environments," *Water Pollution Control Federation Journal*, vol. 47, pp. 135, 1975.

[27] M.K. Hamdy and O.R. Noyes, "Formation of methylmercury by bacteria," *Journal of Applied Microbiology*, vol. 30, pp. 424, 1975.

[28] B.H. Olson and R.C. Cooper, "Comparison of aerobic and anaerobic methylation of mercuric chloride by San Francisco Bay sediments," Water Research, vol. 10, pp. 113, 1976.

[29] G. Compeau and R. Bartha, "Methylation and demethylation of mercury under controlled redox, pH and salinity conditions," *Applied and Environmental Microbiology*, vol. 48, pp. 1203, 1984.

[30] G.C. Compeau and R. Bartha, "Sulfate-reducing bacteria: principal methylators of mercury in anoxic estuarine sediment," *Applied and Environmental Microbiology*, vol. 50, pp. 498, 1985.

[31] G.C. Compeau and R. Bartha, "Effect of salinity on mercury-methylating activity of sulfate-reducing bacteria in estuarine sediments," *Applied and Environmental Microbiology*, vol. 53, pp. 261, 1987.

[32] M. Berman and R. Bartha, "Control of the methylation process in a mercury-polluted aquatic sediment," *Environmental Pollution*, Series B, vol. 11, pp. 41, 1986.

[33] O. Regnell, "The effect of pH and dissolved oxygen levels on methylation and partitioning of mercury in freshwater model systems," *Environmental Pollution*, vol. 84, pp. 7-13, 1994.

[34] T. Fagerström and A. Jernelöv, "Formation of methylmercury from pure mercuric sulfide in aerobic organic sediment," *Water Research*, vol. 5, pp. 121, 1971.

[35] A. Jernelöv and B. Åséll, "The feasibility of restoring mercury-contaminated waters, in: Heavy metals in the aquatic environment," Proceedings of the International Conference held in Nashville, Tennessee, P.A. Krenkel, Ed. *Pergamon Press*, Oxford, December 1973.

[36] P.J. Craig and P.A. Moreton, "Total mercury, methyl mercury and sulphide in river carron sediments," Marine Pollution Bulletin, vol. 14, pp. 408, 1983.

[37] G. Compeau and R. Bartha, "Effects of sear salt anions on the formation and stability of methylmercury," *Bulletin of Environmental Contamination and Toxicology*, vol. 31, pp. 486, 1983.

[38] D.C. Gillespie, "Mobilization of mercury from sediments into guppies," Journal of the Fisheries Research Board of Canada," vol. 29, pp. 1035, 1972.

[39] B.H. Olson and R.C. Cooper, "In situ methylation of mercury by estuarine sediment," *Nature*, vol. 252, pp. 682, 1974.

[40] J.E. Blum and R. Bartha, "Effect of salinity on methylation of mercury," *Bulletin of Environmental Contamination and Toxicology*, vol. 25, pp. 404, 1980.

[41] S. Rothenberg, N. Ramanathan, D. Estrin, T. Harmon, and J. Jay, "A proposed sensor deployment to investigate biogeochemical controls on mercury cycling in Mugu Lagoon, CA," Internet document, http://repositories.cdlib.org/cens/Posters/249/.

[42] T. Mahmood, W.M. Kaiser, R. Ali, M. Ashraf, A. Gulnaz, and Z. Iqbal, "Ammonium versus nitrate nutrition of plants stimulates microbial activity in the rhizosphere," *Plant and Soil*, vol. 277, pp. 233-243, 2005.

[43] S.-M. Lee, J.-Y. Jung, and Y.-C. Chung, "Measurement of ammonia inhibition of microbial activity in biological wastewater treatment process using dehydrogenase assay," *Biotechnology Letters*, vol. 22, pp. 991-994, 2000.

[44] B.D. Hall, G.R. Aiken, D.P. Krabbenhoft, M. Marvin-DiPasquale, and C.M. Swarzenski, "Wetlands as principal zones of methylmercury production in southern Louisiana and the Gulf of Mexico region," *Environmental Pollution*, vol. 154, pp. 124-134, 2008.

[45] L.-J. Jin, P. Guo, and X.-Q. Xu, "Effect of selenium on mercury methylation in anaerobic lake sediments," *Bulletin of Environmental Contamination and Toxicology*, vol. 59, pp. 994-999, 1997.

[46] S.-L. Tong, "Stationary cold-vapor atomic absorption spectrometric method for mercury determination," *Analytical Chemistry*, vol. 50, no. 3, pp. 412-414, May 2002.

[47] H. Emteborg, H.-W. Sinemus, B. Radziuk, D.C. Baxter, and W. Frech, "Gas chromatography coupled with atomic absorption spectrometry – a sensitive instrumentation for mercury speciation," *Spectrochimica Acta Part B*, vol. 51, pp. 829-837, 1996.

[48] J. Szkoda, J. Zmudzki, and A. Grzebalska, "Determination of total mercury in biological material by atomic absorption spectrometry method," *Bulletin of the Veterinary Institute in Pulawy*, vol. 50, pp. 363-366, 2006.

[49] P. Hashemi and A. Rahimi, "A highly sensitive method for the determination of mercury using vapor generation gold wire microextraction and electrothermal atomic absorption spectrometry," *Spectrochimica Acta*, Part B, vol. 62, pp. 423-428, 2007.

[50] Y. Nojiri, A. Otsuki, and K. Fuwa, "Determination of sub-nanogram-per-liter levels of mercury in lake water with atmospheric pressure helium microwave induced plasma emission spectrometry," *Analytical Chemistry*, vol. 58, no. 3, pp. 544-547, May 2002.

[51] Y. Cai, S. Monsalud, and K.G. Furton, "Determination of methyl- and ethylmercury compounds using gas chromatography atomic fluorescence spectrometry following aqueous derivatization with sodium tetraphenylborate," *Chromatographia*, vol. 52, pp. 52-86, 2000.

[52] H. Hintelmann, R. Douglas Evans, and J.Y. Villeneuve, "Measurement of mercury methylation in sediments by using enriched stable mercury isotopes combined with methylmercury determination by gas chromatography-inductively coupled plasma mass spectrometry," *Journal of Analytical Atomic Spectrometry*, vol. 10, pp. 619-624, 1995.

[53] J.A. Shatkin, H.S. Brown, and S. Licht, "Composite graphite ion selective electrode array potentiometry for the detection of mercury and other relevant ions in aquatic systems," *Analytical Chemistry*, vol. 67, no. 6, pp. 1147- 1151, 1995.

[54] M. Korolczuk, "Application of cold vapor differential pulse voltammetric method for determination of mercury in urine samples," *Microchemical Journal*, vol. 57, pp. 81-85, 1997.

[55] P.D. Selid, H. Xu, E.M. Collins, M.S. Face-Collins, and J.X. Zhao, "Sensing mercury for biomedical and environmental monitoring," *Sensors*, vol. 9, pp. 5446-5459, 2009.

[56] I. Bontidean, A. Mortari, S. Leth, N.L. Brown, U. Karlson, M.M. Larsen, J. Vangronsveld, P. Corbisier, and E. Csoregi, "Biosensors for detection of mercury in contaminated soils," *Environmental Pollution*, vol. 131, pp. 255-262, 2004.

[57] P.R.G. Barrocas, "Assessment of mercury (II) species bioavailability using bioluminescent bacterial biosensor," PhD. dissertation, Florida State University, Tallahassee, FL, USA, 2004.

[58] L. Guo, W. Zhang, Z. Xie, X. Lin, and G. Chen, "An organically modified sol-gel membrane for detection of mercury ions by using 5, 10, 15,20-tetraphenylporphyrin as a fluorescence indicator," *Journal of Sensors and Actuators B*, vol. 119, pp. 209-214, 2006.

[59] Y. Zhao, Z. Lin, C. He, H. Wu, and C.A. Duan, ""Turn-on" fluorescent sensor for selective Hg(II) detection in aqueous media based on meta-induced dye formation," *Inorganic Chemistry*, vol. 45, pp. 10013-10015, 2006.

[60] A. Segura-Carretero, J.M. Costa-Fernandez, R. Pereiro, and A. Sanz-Medel, "Low-level mercury determination with thiamine by fluorescence optosensing," *Talanta*, vol. 49, pp. 907-913, 1999.

[61] M.H. Ha-Thi, M. Penhoat, V. Michelet, and I. Leray, "Highly selective and sensitive phosphane sulfide derivative for the detection of Hg^{2+} in an organoaqueous medium," *Organic Letters*, vol. 9, pp. 1133-1136, 2007.

[62] G. Zhang, D. Zhang, S. Yin, X, Yang, Z. Shuai, and D. Zhu, "1,3-dithiole-2-thione derivatives featuring an anthracene unit: new selective chemodosimeters for Hg(II) ion," *Chemical Communications*, pp. 2161-2163, 2005.

[63] J. Holzbecher and D.E. Ryan, "The fluorimetric determination of mercury," *Analytica Chimica Acta*, vol. 64, pp. 333-336, 2005.

[64] M.A. Ryan and J.D. Ingle Jr., "Fluorometric reaction tate method for the determination of thiamine," *Analytical Chemistry*, vol. 52, pp. 2177-2187, 1980.

[65] K. Schambach, K. Eden, K. Schumacher, and G. Wiegleb, "Micromachined Mercury Sensor," *Proceedings of the 30th European Solid-State Device Research Conference (ESSDERC'02)*, pp. 443-446, 2002.

[66] J.J. McNerney, P.R. Buseck, and R.C. Hanson, "Mercury detection by means of thin gold films," *Science Magazine*, vol. 178, no. 4061, pp. 611-612, November 1972.

[67] C. Battistoni, E. Bemporad, E. Galdikas, S. Kaciulis, G. Mattogno, S. Mickevicius, and V. Olevano, "Interaction of mercury vapour with thin films of gold," *Applied Surface Science*, vol. 103, pp. 107-111, 1996.

[68] M. Levlin, E. Ikavalko, and T. Laitinen, "Adsorption of mercury on gold and silver surfaces," *Fresenius' Journal of Analytical Chemistry*, vol. 365, pp. 577-586, 1999.

[69] A.V. Shevade, M.L. Homer, H. Zhou, A.D. Jewell, A.K. Kisor, K.S. Manatt, J. Torres, J. Soler, S.-P.S. Yen, M. Blanco, W.A. Goddard, and M.A. Ryan, "Development of the third generation JPL electronic nose for international space station technology demonstration," *SAE Transactions Journal of Aerospace*, vol. 1, pp. 3149-3156, 2007.

[70] L. Bennun and J. Gomez, "Determination of mercury by total-reflection x-ray fluorescence using amalgamation with gold," *Spectrochimica Acta Part B*, vol. 52, pp. 1195-1200, 1997.

[71] C.C. Huang and H.T. Chang, "Selective gold-nanoparticle-based "Turn-on" fluorescent sensors for detection of mercury(II) in aqueous solution," *Analytical Chemistry*, vol. 78, pp. 8332-8338, 2006.

[72] J. Chen, A. Zheng, A. Chen, Y. Gao, C. He, X. Kai, G. Wu, and Y. Chen, "A functionalized gold nanoparticles and Rhodamine 6G based fluorescent sensor for high sensitive and selective detection of mercury(II) in environmental water samples," *Analytica Chemica Acta*, vol. 599, pp. 134-142, 2007.

[73] J. Drelich, C.L. White, and Z. Xu, "Laboratory tests on mercury emission monitoring with resonating gold-coated silicon cantilevers," *Environmental Science & Technology*, vol. 42, pp. 2072-2078, 2008.

[74] B. Rogers, L. Manning, M. Jones, T. Sulchek, K. Murray, B. Beneschott, J.D. Adams, Z. Hu, T. Thundat, H. Cavazos, and S.C. Minne, "Mercury vapor detection with a self-sensing, resonating piezoelectric cantilever," *Review of Scientific Instruments*, vol. 74, no. 11, pp. 4899-4901, November 2003.

[75] X. Xu, T.G. Thundat, G.M. Brown, and H.-F. Ji, "Detection of Hg^{2+} using microcantilever sensors," *Analytical Chemistry*, vol. 74, pp. 3611-3615, August 2002.

[76] C. Vancura, M. Ruegg, Y. Li, C. Hagleitner, and A. Hierlemann, "Magnetically actuated complementary metal oxide semiconductor resonant cantilever gas sensor systems," *Analytical Chemistry*, vol. 77, pp. 2690-2699, 2005.

[77] F. Quist, V. Tabard-Cossa, and A. Badia, "Nanomechanical cantilever motion generated by a surface-confined redox reaction," *Journal of Physical Chemistry B*, vol. 107, pp. 10691-10695, 2003.

[78] T. Thundat, E.A. Wachter, S.L. Sharp, and R.J. Warmack, "Detection of mercury vapour using resonating microcantilevers," *Applied Physics Letters*, vol. 66, pp. 1675-1697, 1995.

[79] G. Liu, Y. Lin, Y. Tu, and Z. Ren, "Ultrasensitive voltammetric detection of trace heavy metal ions using carbon nanotube nanoelectrode array," *Analyst*, vol. 130, pp. 1098-1101, 2005.

[80] S. Keebaugh, A.K. Kalkan, W.J. Nam, and S.J. Fonash, "Gold nanowires for the detection of elemental and ionic mercury," *Electrochemical and Solid-State Letters*, vol. 9, pp. H88-H91, 2006.

[81] J.J. Caron, R.B. Haskell, D.G. Libby, C.J. Freeman, and J.F. Vetelino, "A surface acoustic wave mercury vapor sensor," *Proceedings of the IEEE International Frequency Control Symposium*, 1997.

[82] M.G. Schweyer, J.C. Andle, D.J. McAllister, and J.F. Vetelino, "An acoustic plate mode sensor for aqueous mercury," *Sensors and Actuators B*, vol. 35-36, pp. 170-175, 1996.

[83] L. Rufer, T. Lalinsky, D. Grobelny, S. Mir, G. Vanko, Z. Oszi, Z. Mozolova, and J. Gregus, "GaAs and GaN based SAW chemical sensors: acoustic part design and technology," *The 6th International Conference on Advanced Semiconductor Devices and Microsystems (ASDAM'06)*, pp. 165-168, Smolenice, Slovakia, October 16-18, 2006.

[84] L. Spassov, D.Y. Yankov, A.N. Mogilevski, and A.D. Mayorov, "Piezoelectric sorption sensor for mercury vapors in air using a quartz resonator," *Review of Scientific Instruments*, vol. 64, pp. 225, 1993.

[85] D.P. Ruys, J.F. Andrade, and O.M. Guimaraes, "Mercury detection in air using a coated piezoelectric sensor," *Analytica Chemica Acta*, vol. 404, pp. 95-100, 2000.

[86] L. Manganiello, A. Rios, and M.A. Valcarcel, "Method for screening total mercury in water using a flow injection system with piezoelectric detection," *Analytical Chemistry*, vol. 74, pp. 921-925, 2002.

[87] U.S. Environmental Protection Agency (EPA), "Mercury," Internet document, http://www.epa.gov/mercury/.

[88] Y. Mao, G. Liu, G. Meichel, Y. Cai, and G. Jiang, "Simultaneous speciation of monomethylmercury and monoethylmercury by aqueous phenylation and purge-and-trap preconcentration followed by atomic spectrometry detection," *Analytical Chemistry*, vol. 80, pp. 7163-7168, 2008.

[89] M. Matsushita, M.M. Meijler, P. Wirsching, R.A. Lerner, and K.D. Janda, "A blue fluorescent antibody-cofactor sensor for mercury," *Organic Letters*, vol. 7, pp. 4943-4946, 2005.

[90] M.A. Ryan, M.L. Homer, A.V. Shevade, L.M. Lara, S.-P.S. Yen, A.K. Kisor, and K.S. Manatt, "Conductometric sensor for detection of elemental mercury vapor," *ECS Transactions*, vol. 16, pp. 431-439, 2008.

[91] M. Rex, F.E. Hernandez, and A.D. Campiglia, "Pushing the limits of mercury sensors with gold nanorods," *Analytical Chemistry*, vol. 78, pp. 445-451, 2006.

[92] L. Spassov, D.Y. Yankov, A.N. Mogilevski, and A.D. Mayorov, "Piezoelectric sorption sensor for mercury vapors in air using a quartz resonator," *Review of Scientific Instruments,* pp. 225-227, January 2003.

[93] K. Schambach, K. Eden, K. Schumacher, and G. Wiegleb, "Micromachined mercury sensor," *Proceedings of the 30th European Solid-State Device Research Conference (ESSDERC'02,)* pp. 443-446, 2002.

[94] I. Biran, D.M. Rissin, E.Z. Ron, and D.R. Walt, "Optical imaging fiber-based live bacterial cell array biosensor," *Analytical Biochemistry*, vol. 315, pp. 106-113, 2003.

APPENDIX A.

Identification information for each of the chemicals and materials utilized throughout project experimentation are as follows:

1. Citric Acid (Monohydrate, Granular) – $HO_2C(OH)C(CH_2CO_2H)_2 \cdot H_2O$, (Vendor) EM, CAT # CX1725-1 500G, Batch # 8005.
2. Hydrochloric Acid, Certified A.C.S. Plus – HCl, (Vendor) Fischer Scientific, CAT # A144S-212, CAS # FL-08-0499.
3. Methylmercury (II) Chloride standard solution, 1.0 μg/mL by CVAFS in 0.5% HOA_C, 0.2% HCl – $(CH_3HgCl)_2$, (Vendor) Brooks Rand Labs, Analysis Lot # 1012011, Expiration: 04/26/2011, PN 06610.
4. Potassium Bromate – $KBrO_3$, (Vendor) Sigma-Aldrich, CAT # 309087-100G, CAS # 7758-01-2, Batch # 06116CD.
5. Postassium Bromide – KBr, (Vendor) Aldrich, CAT # 24, 341-8, CAS # 7758-02-3, LOT # 02827DG.
6. Quartz Wool 10g – (Vendor) Alltech, CAT# 4033, LOT # 05H7, Batch # 3111973.
7. Sodium Citrate – $C_6H_5Na_3O_7 \cdot 2H_2O$, (Vendor) Sigma, CAT # S1804-500G, CAS # 6132-04-3, Batch # 097K0017.
8. Sodium Chloride – NaCl, (Vendor) Sigma, CAT # S9625-500G, CAS # 7647-14-5, Batch # 038K0045.
9. Sodium Chloride – NaCl, (Vendor) Sigma, CAT # S-9888, CAS # 7647-14-5, LOT # 49H0251, EC # 231-598-3.
10. Sodium Tetraphenylborate – C24H2oB, (Vendor) Sigma-Aldrich, CAT # T25402-25G, CAS # 143-66-8, LOT # 05627EJ, EC # 205-605-5.
11. Tin (II) Chloride Dihydrate – $SnCl_2 \cdot 2H_2O$, (Vendor) Fischer Scientific, CAT # T142-500, CAS # 10025-69-1, LOT # 093481.
12. Tin (II) Chloride Dihydrate – $SnCl_2 \cdot 2H_2O$, (Vendor) Aldrich, CAT # 431508-50G, CAS # 10025-69-1, Batch # 09106TA.

APPENDIX B.

Frequency responses from various experimental runs for Stage #1 is shown as follows:

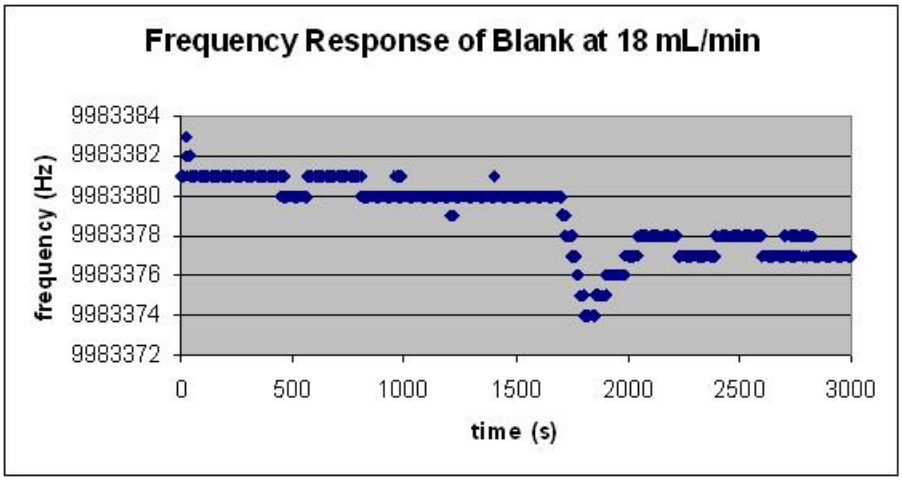

Figure 34 – Frequency response of blank at 18 mL/min using polished QCM sensor.

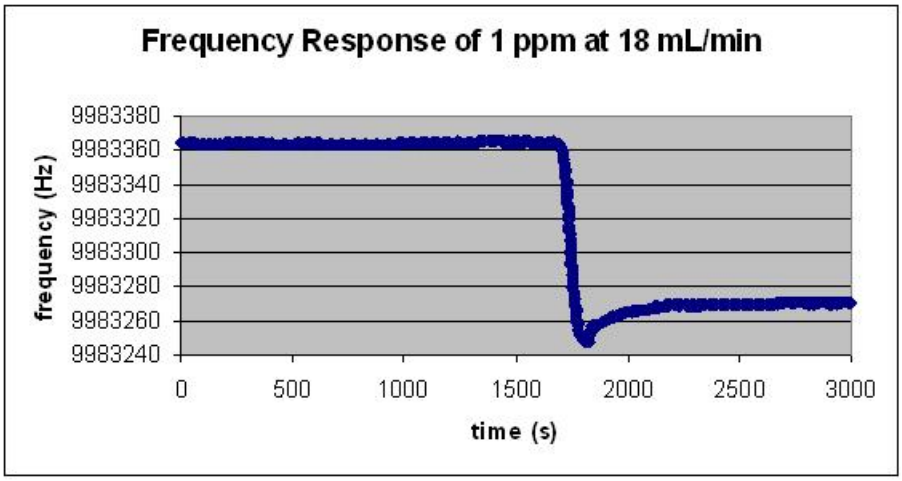

Figure 35 – Frequency response of 1 ppm at 18 mL/min using polished QCM sensor.

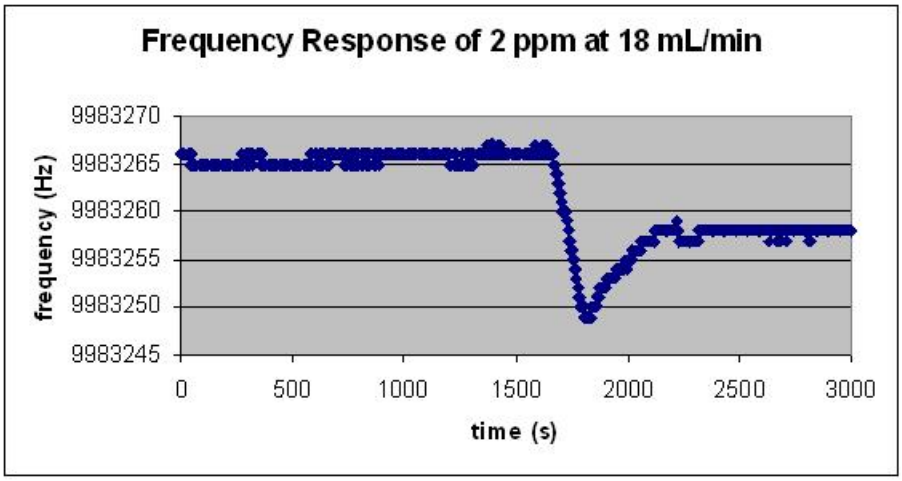

Figure 36 – Frequency response of 2 ppm at 18 mL/min using polished QCM sensor.

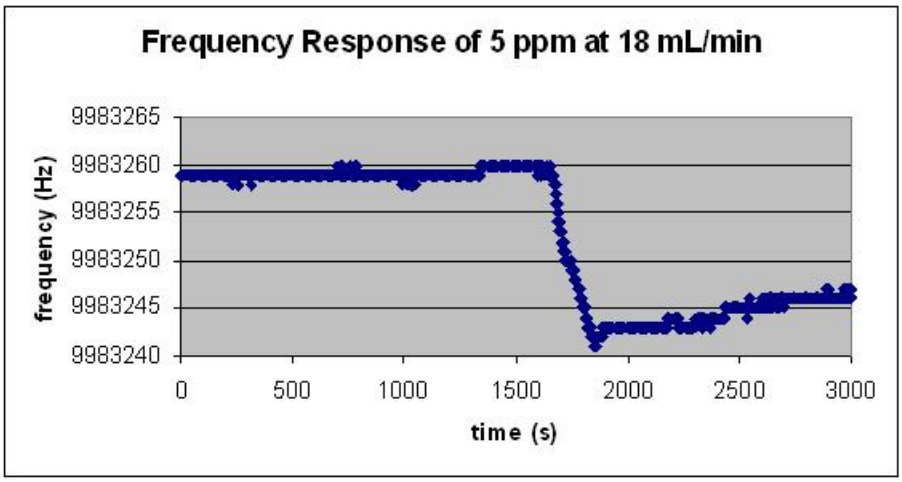

Figure 37 – Frequency response of 5 ppm at 18 mL/min using polished QCM sensor.

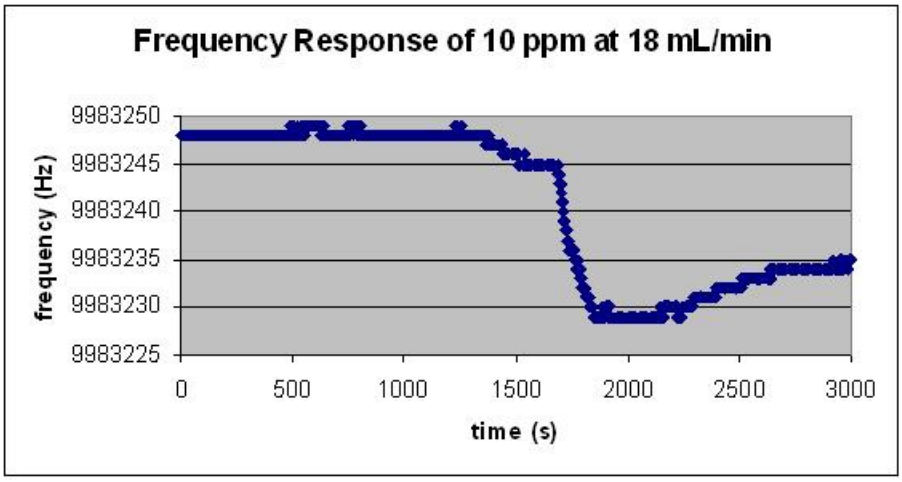

Figure 38 – Frequency response of 10 ppm at 18 mL/min using polished QCM sensor.

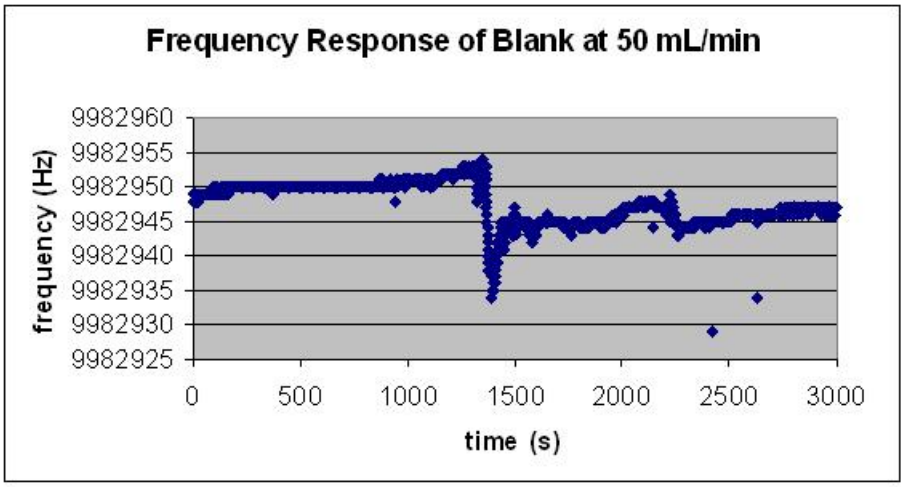

Figure 39 – Frequency response of blank at 50 mL/min using polished QCM sensor.

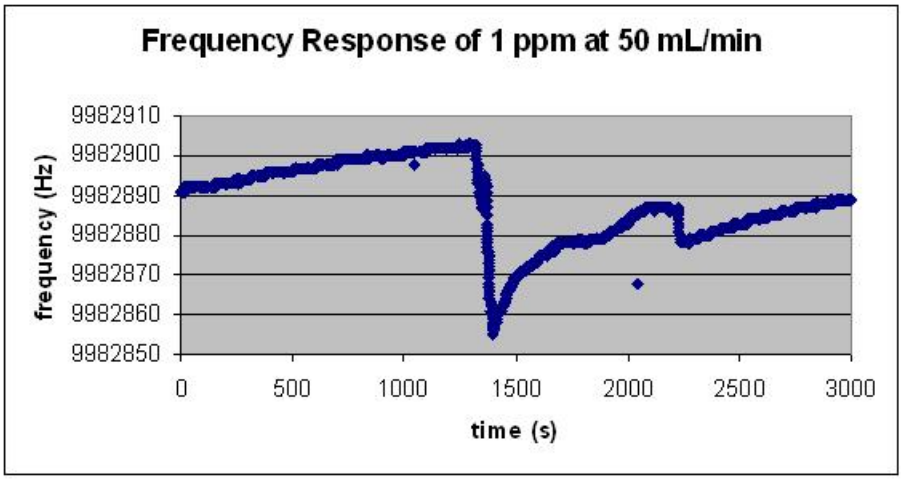

Figure 40 – Frequency response of 1 ppm at 50 mL/min using polished QCM sensor.

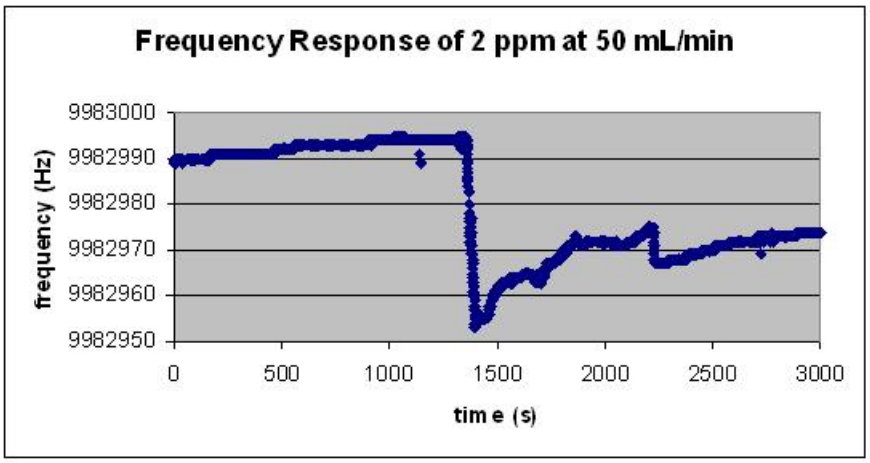

Figure 41 – Frequency response of 2 ppm at 50 mL/min using polished QCM sensor.

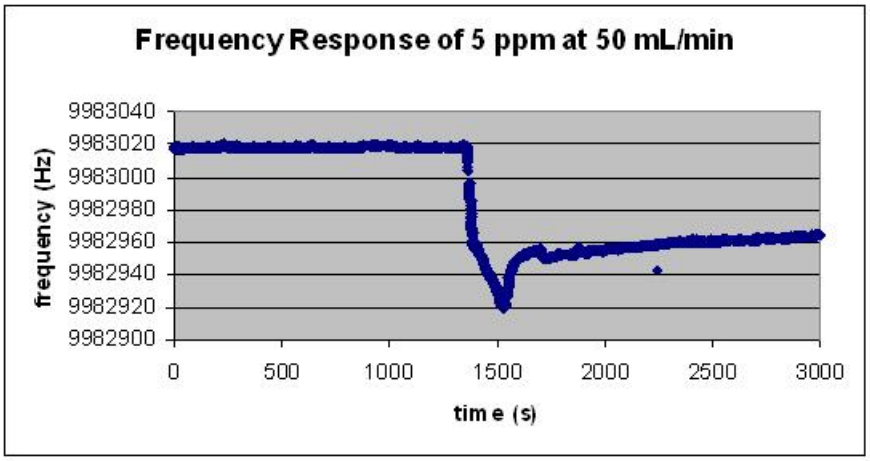

Figure 42 – Frequency response of 5 ppm at 50 mL/min using polished QCM sensor.

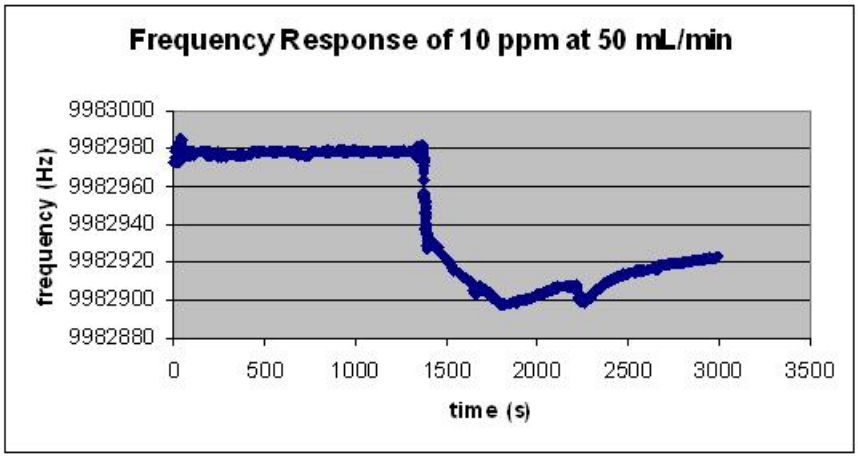

Figure 43 – Frequency response of 10 ppm at 50 mL/min using polished QCM sensor.

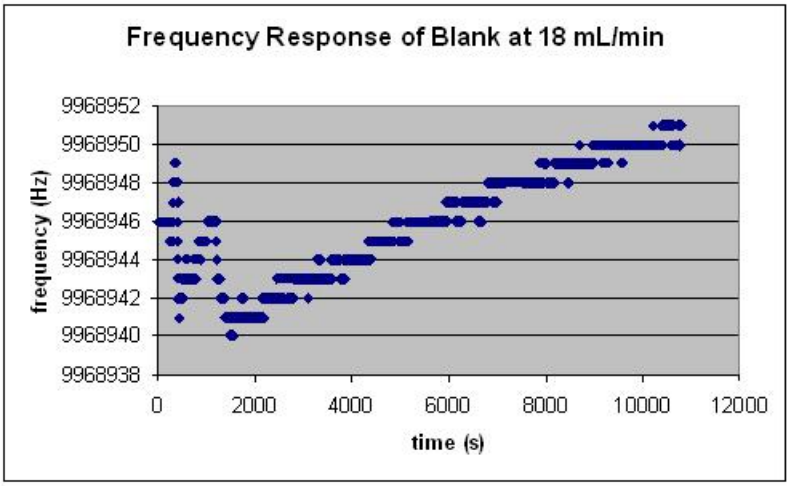

Figure 44 – Frequency response of blank at 18 mL/min using etched QCM sensor.

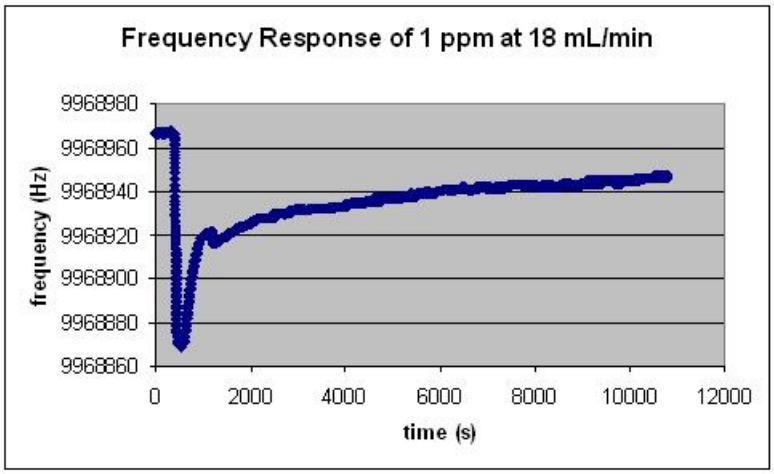

Figure 45 – Frequency response of 1 ppm at 18 mL/min using etched QCM sensor.

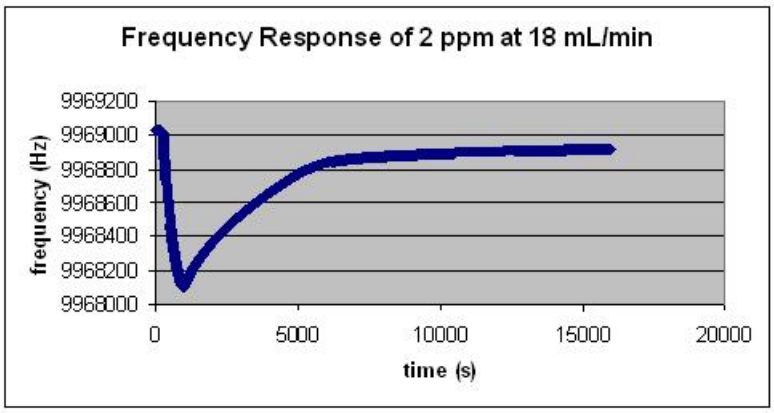

Figure 46 – Frequency response of 2 ppm at 18 mL/min using etched QCM sensor.

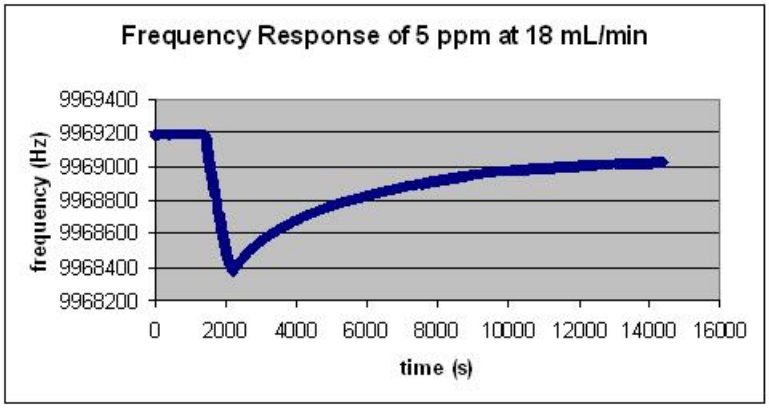

Figure 47 – Frequency response of 5 ppm at 18 mL/min using etched QCM sensor.

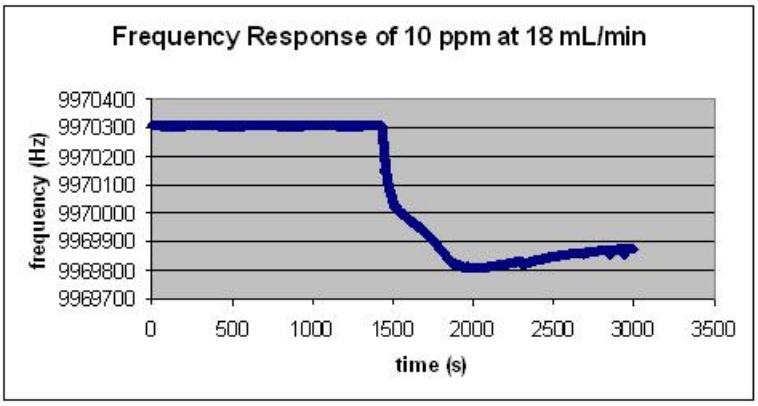

Figure 48 – Frequency response of 10 ppm at 18 mL/min using etched QCM sensor.

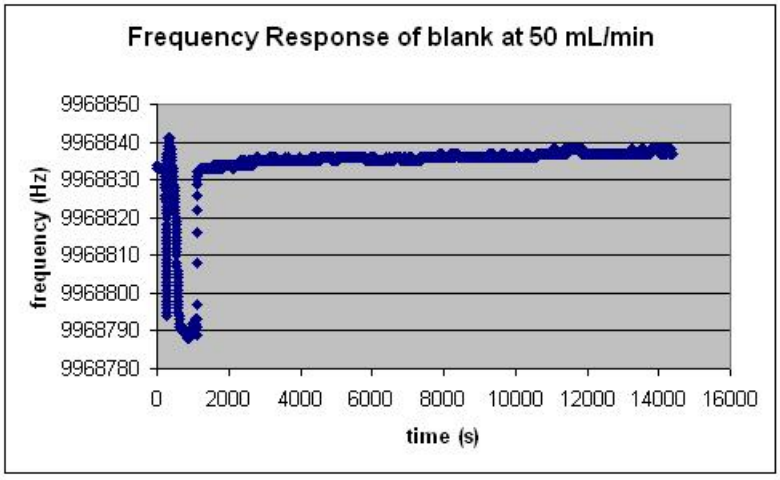

Figure 49 – Frequency response of blank at 50 mL/min using etched QCM sensor.

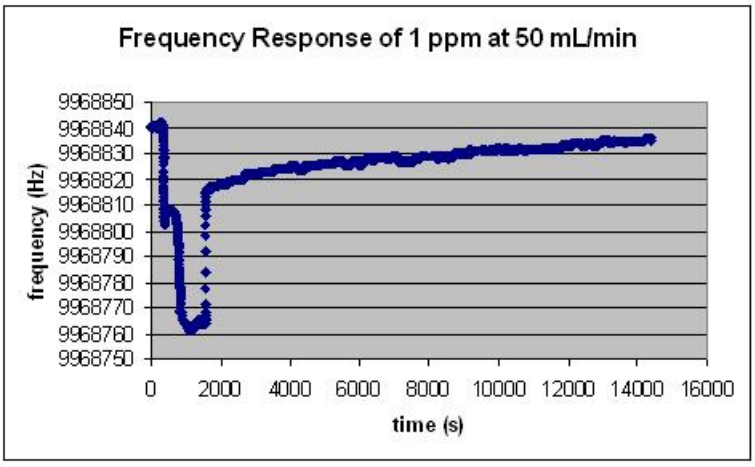

Figure 50 – Frequency response of 1 ppm at 50 mL/min using etched QCM sensor.

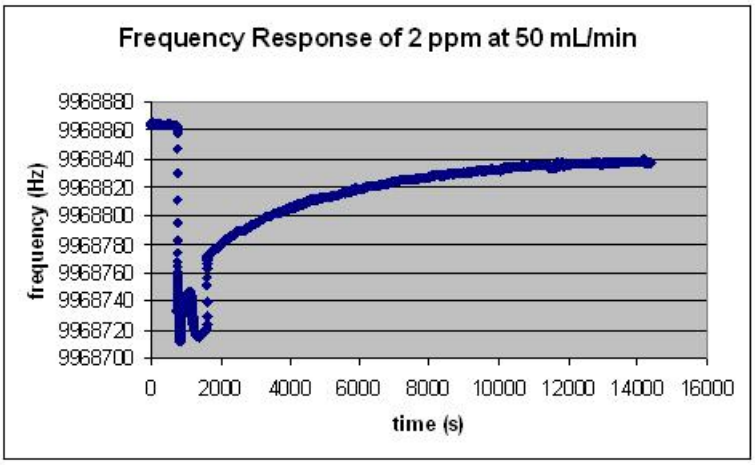

Figure 51 – Frequency response of 2 ppm at 50 mL/min using etched QCM sensor.

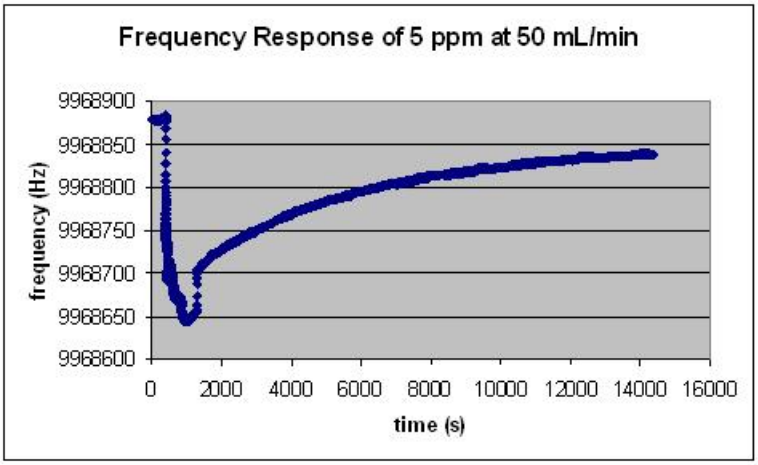

Figure 52 – Frequency response of 5 ppm at 50 mL/min using etched QCM sensor.

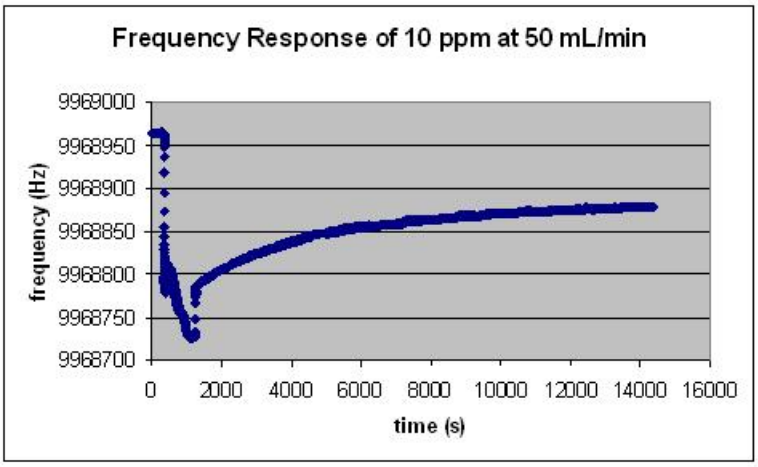

Figure 53 – Frequency response of 10 ppm at 50 mL/min using etched QCM sensor.

APPENDIX C.

Frequency responses from various experimental runs for Stage #2 is shown as follows:

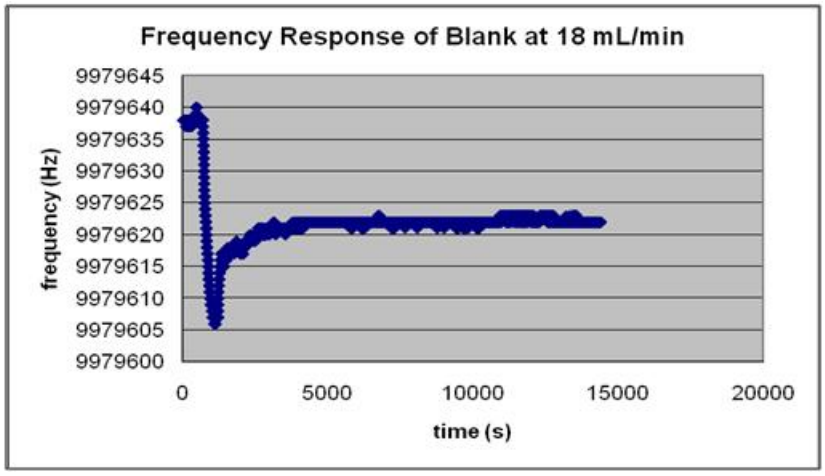

Figure 54 – Frequency response of blank at 18 mL/min.

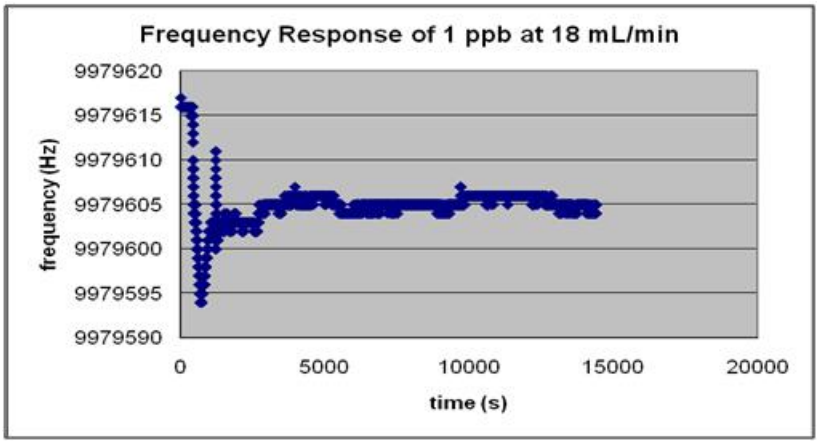

Figure 55 – Frequency response of 1 ppb at 18 mL/min.

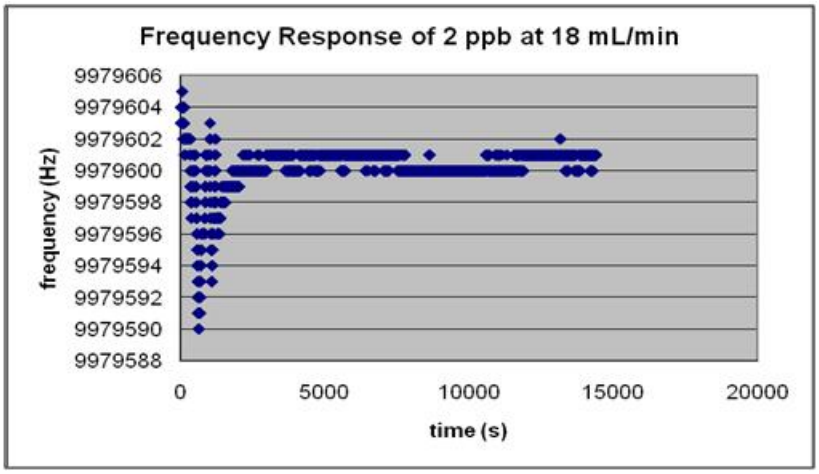

Figure 56 – Frequency response of 2 ppb at 18 mL/min.

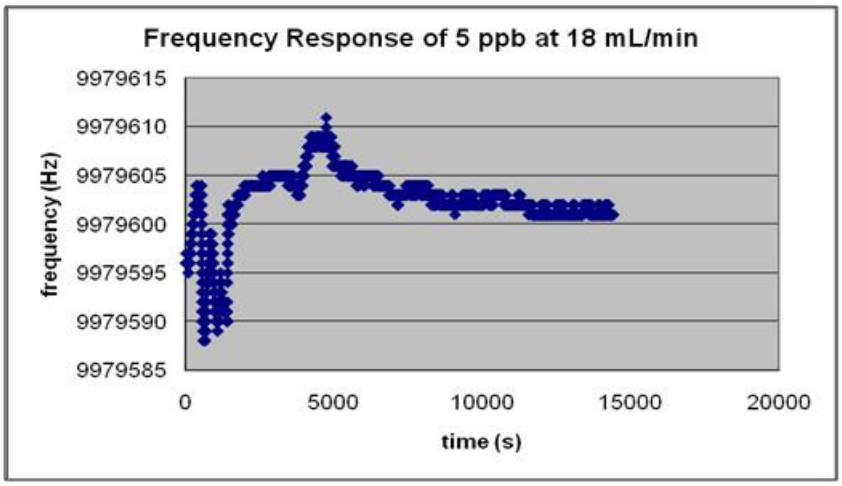

Figure 57 – Frequency response of 5 ppb at 18 mL/min.

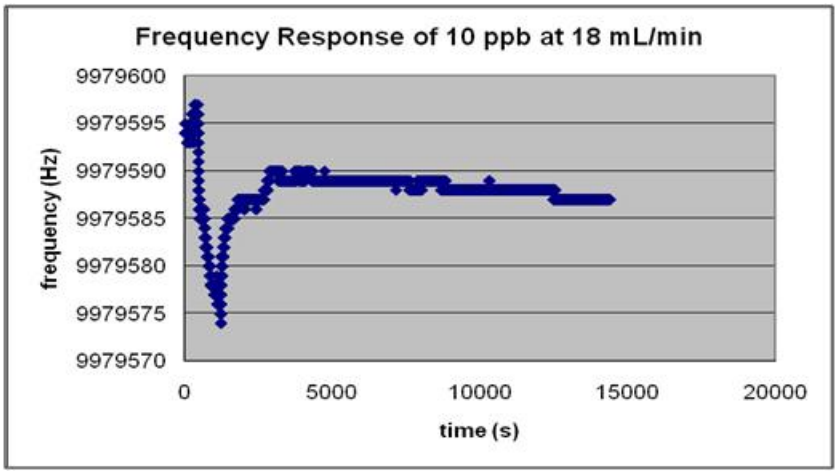

Figure 58 – Frequency response of 10 ppb at 18 mL/min.

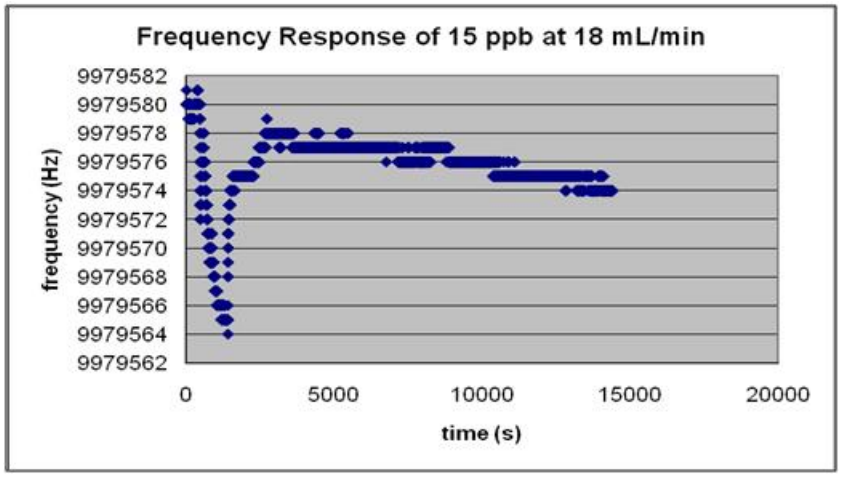

Figure 59 – Frequency response of 15 ppb at 18 mL/min.

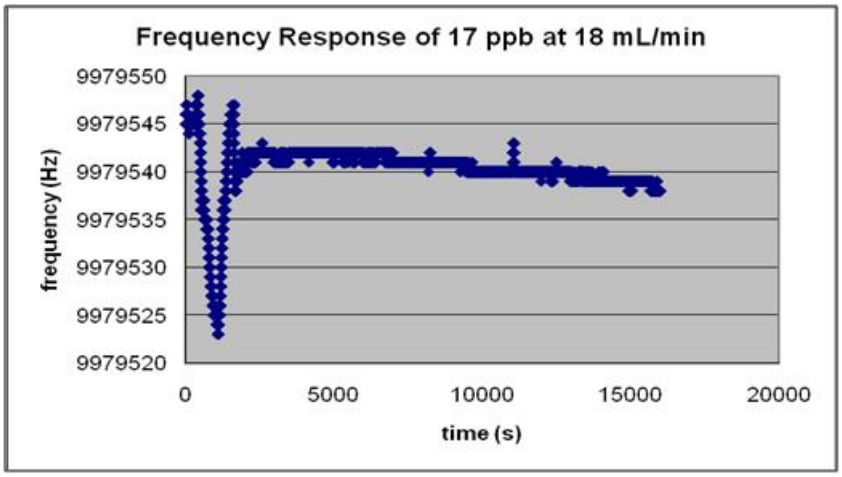

Figure 60 – Frequency response of 17 ppb at 18 mL/min.